Review Article

Huiyu Duan, Tong Wang, Ziyun Su, Huan Pang*, and Changyun Chen*

Recent progress and challenges in plasmonic nanomaterials

https://doi.org/10.1515/ntrev-2022-0039 received July 23, 2021; accepted January 4, 2022

Abstract: Owing to their optical, mechanical, and catalytic properties, plasmonic nanomaterials (P-NMs) have been widely used in sensing, disease treatment, as well as energy transfer and conversion applications. Therefore, the synthesis, properties, and applications of P-NMs have garnered significant interest in recent decades. This review surveys the various types of P-NMs, their synthesis methods, their properties, and recent applications. In addition, we summarize the current challenges and future developments in P-NMs. We hope this article will help researchers to gain a deeper understanding of P-NM applications in the field of energy, overcome the current problems associated with P-NMs, and develop novel P-NMs with better characteristics.

Keywords: nanomaterial, noble metal, plasmon, plasmonic nanomaterial

1 Introduction

Recent development in advanced processing and characterization approaches have boosted the research on nanomaterials [1–16]. Nanoscale materials have some advantageous acoustic, optical, electrical, magnetic, and thermal characteristics,

* Corresponding author: Huan Pang, School of Chemistry and Chemical Engineering, Institute for Innovative Materials and Energy, Yangzhou University, Yangzhou, 225009, Jiangsu, China, e-mail: huanpangchem@hotmail.com

Huiyu Duan: Key Laboratory of Advanced Functional Materials of Nanjing, School of Environmental Science, Nanjing Xiaozhuang University, Nanjing, 211171, Jiangsu, China; School of Chemistry and Chemical Engineering, Institute for Innovative Materials and Energy, Yangzhou University, Yangzhou, 225009, Jiangsu, China Tong Wang, Ziyun Su: Key Laboratory of Advanced Functional Materials of Nanjing, School of Environmental Science, Nanjing Xiaozhuang University, Nanjing, 211171, Jiangsu, China

which make them potentially applicable in many fields (e.g., energy storage and conversion [17-31] and medical treatment and transportation [32–37]). However, owing to their small size, these materials often exhibit defects and some nondesirable features, such as high surface energy and easy agglomeration, making them nonconducive to long-term storage [38-42]. These drawbacks have significantly hindered the adoption of nanomaterials for practical applications. To alleviate these drawbacks, coping strategies have been sought by many researchers. Feichtenschlager et al. used hydrothermal methods for preparing ZrO2 nanocrystals and modified the surfaces of nanocrystals using coating agents [43]. They found that after such surface modification, the molecular structure of the studied ZrO₂ nanocrystals changed significantly. At the same time, the agglomeration behavior of these nanocrystals improved, and the overall performance of the coated materials improved as well. In addition to surface modification strategies, two major strategies have been proposed: (1) innovative synthesis methods and (2) doping based on nanomaterials. Pan and coworkers dispersed nanoparticles (NPs) in a volatile solvent and mixed them with an uncured polymer precursor, obtaining a microemulsion [44]. Those NPs were then quickly evaporated to prevent NP agglomeration during the polymer curing stage. This method eliminates the need for NP surface functionalization. It is suitable for preparing nanocomposites (NCs) of various polymers and is promising for novel NCs with novel functions.

To further stimulate the performance of nanomaterials and develop their applications, researchers have proposed a novel family of nanomaterials – plasmonic nanomaterials (P-NMs) [45–56]. Plasmons can be described in the classical picture as an oscillation of electron density with respect to the fixed positive ions in a metal. To visualize a plasma oscillation, imagine a cube of metal placed in an external electric field pointing to the right. Electrons will move to the left side (uncovering positive ions on the right side) until they cancel the field inside the metal. If the electric field is removed, the electrons move to the right, repelled by each other and attracted to the positive ions left bare on the right side. They oscillate back and forth at

^{*} Corresponding author: Changyun Chen, Key Laboratory of Advanced Functional Materials of Nanjing, School of Environmental Science, Nanjing Xiaozhuang University, Nanjing, 211171, Jiangsu, China, e-mail: cychen@njxzc.edu.cn

the plasma frequency until the energy is lost in some kind of resistance or damping. Plasmons are a quantization of this kind of oscillation. Surface plasmons are those plasmons that are confined to surfaces and that interact strongly with light resulting in a polariton. They occur at the interface of a material exhibiting positive real part of their relative permittivity, that is, dielectric constant (e.g., vacuum, air, glass, and other dielectrics) and a material whose real part of permittivity is negative at the given frequency of light, typically a metal or heavily doped semiconductor. In addition to opposite sign of the real part of the permittivity, the magnitude of the real part of the permittivity in the negative permittivity region should typically be larger than the magnitude of the permittivity in the positive permittivity region, otherwise the light is not bound to the surface. The particular choice of materials can have a drastic effect on the degree of light confinement and propagation distance due to losses. Surface plasmons can also exist on interfaces other than flat surfaces, such as particles, or rectangular strips, v-grooves, cylinders, and other structures. Many structures have been investigated due to the capability of surface plasmons to confine light below the diffraction limit of light.

Compared with the ordinary nanomaterials, P-NMs exhibit a better performance, and their use has led to many novel results in many applications [57-63]. P-NMs consist of cations and free electrons that are present on the surface of the materials. The free electrons collectively oscillate under the action of the photoelectric field. Because of this effect, P-NMs can be activated and yield hot electrons, which makes these materials catalytically active. In addition, the cations and free electrons on the P-NM surfaces can form plasmonic waves, which in turn enhances the light field, resulting in the surface plasmon resonance (SPR) effect. local SPR (LSPR) effect, surface-enhanced Raman scattering (SERS), plasmon resonance energy transfer (PRET), and magneto-optical (MO) effects. These effects further improve the performance of P-NMs; as a result, P-NMs have garnered significant attention.

In the continuing process of exploration and research, researchers have developed many P-NMs with novel and exciting properties. Examples include metal-based P-NMs, carbon-based P-NMs, sulfur-based P-NMs, and plasmonic active-structure nanofilms [64–77]. Among these, metal-based P-NMs and carbon-based P-NMs have attracted the most attention. Metal-based P-NMs exhibit excellent physical and chemical properties. Among the most striking are their plasmon optical properties, which prompted many researchers to study them. Ma *et al.* used a simple one-pot synthesis method for constructing core—shell (CS) gold nanorod@layered double hydroxide (GNR@LDH) nano-

materials (Figure 1a) with good photothermal conversion rates [78]. This excellent performance was attributed to the electron transfer of the upper part of gold (Au) in GNR@LDH, which caused the CS GNR@LDH and layered double hydroxides to have more electron interactions and enhanced the plasmonic absorption effect. The development of this CS GNR@LDH material has established a platform for light-to-heat conversion, antibacterial, tumor therapy, and bioimaging applications. In addition, owing to its good stability and high electrical conductivity, carbon is becoming increasingly valuable for carbon-based P-NMs. Among these, graphite and carbon nanotubes (CNTs) are the two most commonly used carbon-based nanomaterials. Owing to the rich functional groups on the surface of graphene, it has good electrical conductivity, mechanical strength, thermal conductivity, and stability; as a result, it has been widely studied by many researchers. Primo et al. summarized the P-NMs that were prepared by combining biomolecules with different graphite-derived materials [79]. A series of graphene-derived materials, such as graphene oxide (GO), chitosan (CHIT)-modified graphene (GO-CHIT), and chemical reduction GO-CHIT (RGO-CHIT) were reviewed. The covalent immobilization of Au surfaces modified by different graphene-derived materials on solid substrates was discussed. These materials were shown to exhibit excellent SPR effects and are likely to be helpful in the development of biosensors.

At present, the commonly used methods for synthesizing P-NMs include the solvothermal, microwave-assisted synthesis, chemical deposition, self-assembly, and in situ growth methods. Klinghammer et al. used the electrochemical method for depositing Au on the nanopores of an anodized aluminum oxide (AAO) matrix, and then studied their plasmon characteristics [80]. Figure 1b-d show the related tests that were performed for studying these characteristics. Figure 1b shows that this microbiosensor device relies on a large array of Au nanoantennas. The scanning electron microscopy (SEM) image in Figure 1c confirms that vertically aligned nanoantennas are evenly and densely distributed on the substrate. Figure 1d shows the extinction spectra of nanoantennas with different aspect ratios, measured at different positions on the same sample. The synthesis process of this method is simple, easy to implement, flexible, and easy to convert; the disadvantage is that the voltage and current may be unstable, resulting in an uneven preparation of nanomaterials, which affects the performance. Compared with the electrochemical deposition method, the solvothermal method has the advantages of low energy consumption, less agglomeration, and controllable particle shape. Javed et al. successfully synthesized the silver (Ag)/rGO/TiO₂ ternary NCs using the solvothermal

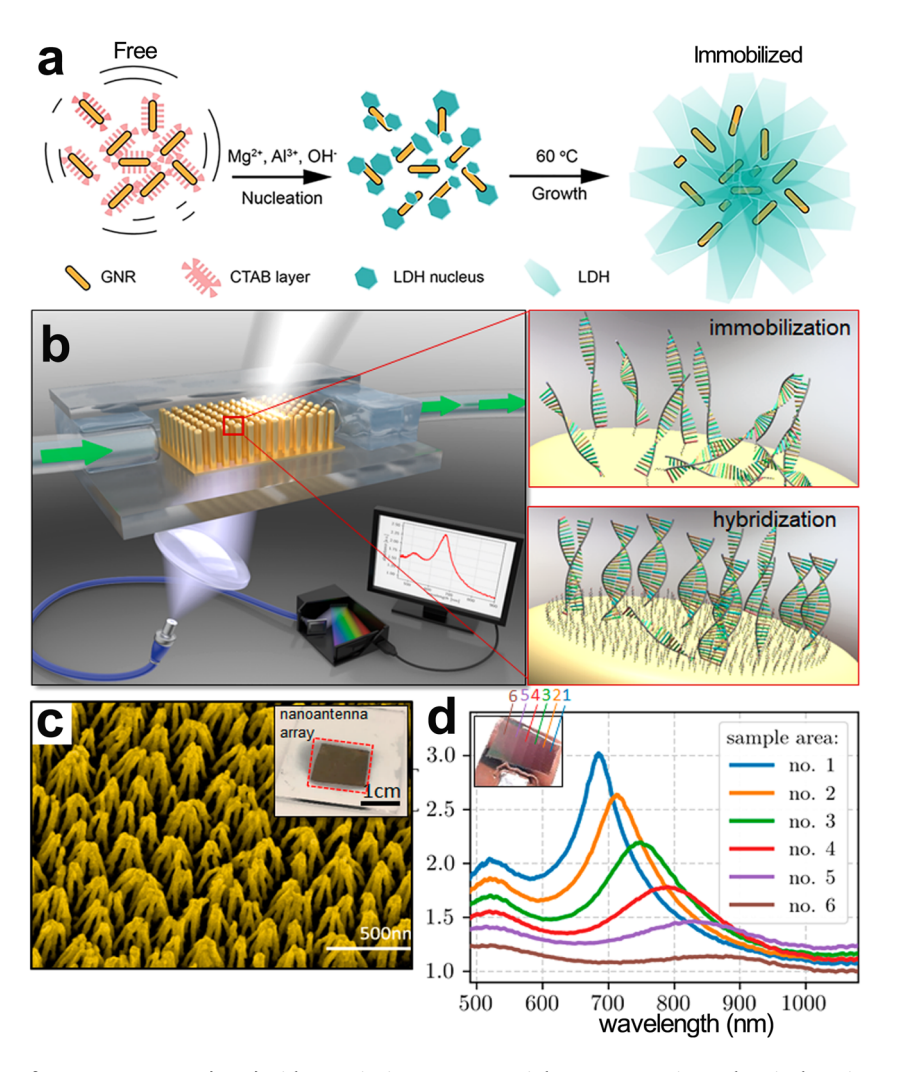


Figure 1: (a) Synthesis of GNR@LDH, reproduced with permission [78]. Copyright 2019, American Chemical Society. (b) Representative drawing of the LSPR-based biosensor for real-time detection; (c) SEM images of vertically aligned nanoantennas. (d) extinction spectra of nanoantennas with different aspect ratios measured at different spots on one and the same sample, reproduced with permission [80]. Copyright 2018, American Chemical Society.

method for high-efficiency plasmonic dye-sensitized solar cells (PDSSCs) [81]. However, the disadvantage is that the yield is low, and the uniformity of the size and morphology of the nanomaterials are not satisfactory. In light of this, the in situ growth method has been generating more interest. Owing to its advantages of morphological controllability and stability, the in situ growth method can yield a variety of nanostructures. Therefore, these nanostructures (such as NPs, nanorods [NRs], nanobeams, nanosheets, nanospheres, and shell cores) have also been extensively studied. In addition, researchers have attempted to develop novel methods to further improve the performance of P-NMs. Ji and coworkers used cation exchange-enabled nonepitaxial strategy to obtain Au@Cu_{2-x}S with controllable CS structure (Figure 2a). Based on experimental and theoretical studies, the aqueous dispersions of as-prepared Au@Cu_{2-x}S NCs have been confirmed with resonant and

off-resonant SPR coupling in both the near infrared (NIR)-I (750–900 nm) and NIR-II region (1,000–1,400 nm). The photothermal conversion efficiency of them can be as high as 43.25% even under 1,064 nm light irradiation. It happens that there is a similar case [36]. Lee *et al.* developed a novel synthesis method (Figure 2b) using sulfide combined with cation exchange, obtaining a heterostructure with plasmonic metal-semiconductor hybridization: Au nanorod-CdS yolk–shell nanostructures (AuNR-CdS YSNs) [82]. During the experiment, it was found that the key to successful synthesis was the exchange of anions and cations.

In addition, Scarabelli *et al.* developed a method for forming a superlattice of Au NRs aligned from the bottom to the top [83]. Under the illumination by light, the structure exhibited an ultraefficient plasmonic effect. It is worth noting that during this growth process, the agglomeration of colloidal particles was caused by the drying solvent.

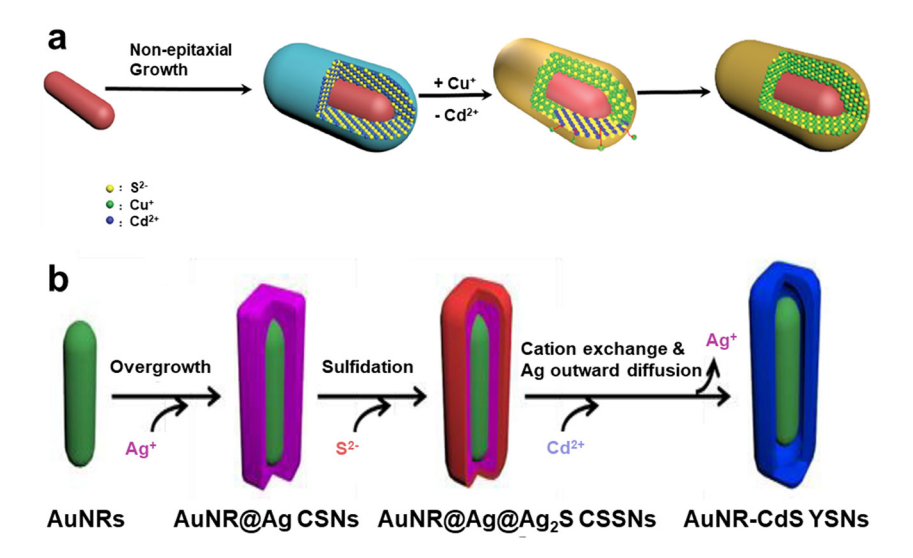


Figure 2: (a) Synthesis scheme of $Au@Cu_{2-x}S$ CS NCs by cation exchange between Au@CdS nanocubes and Cu^+ [36], reproduced with permission. Copyright 2020, American Chemical Society. (b) Schematic of the synthesis route of AuNR-CdS YSNs [82], reproduced with permission. Copyright 2018, Royal Society of Chemistry.

Supercrystals near the edge of the dry solvent usually contain more NRs and stacked layers, whereas the supercrystal in the center is composed of upright NRs composed of a single layer, causing unevenness of the substrate. This hinders the rapid transmission of active channels and electrons, causing changes in their characteristic spectra. It was found that agglomeration negatively affects not only nanomaterials, but also P-NMs. To alleviate this effect to the maximal possible extent, researchers have developed several substrate optimization methods to obtain more homogeneous substrates. At present, the main improvement measures amount to using biologically active substrates, electron beam etching technology, the nanosphere template method, and other nontraditional technologies [84]. Jeong et al. adopted the electron beam etching technology, using a simple oxygen plasmon-etching process to sinter porous Au nanoshells for controlling the nanogaps between the particles, and successfully exfoliated the obtained nanomaterials into a single nanotriangular structure, reducing the reunion effect [85]. The apex of the synthesized material had sharp edges, allowing to concentrate the light field in a narrow gap, which made the plasmon between the needle tip and the shell hybrid further increasing the local electric field and enhancing the SERS effect.

It was found that among all of the effects of P-NMs, the enhancement of SERS and LSPR effects can significantly improve the performance of P-NMs. This is because the SERS and LSPR effects strongly depend on the material's morphology, size, and composition, and even on interparticle gaps. Therefore, the microscopic composition

of NPs can be studied by acquiring and analyzing SPR spectra. When a synthesized NC material is excited by a light source, the formed plasmon thermal electrons can be transferred to the NC material. It can increase the number of catalytically active sites, enhance the charge density inside the material, and improve the electron transport speed to improve the photocatalytic performance. Zhang et al. prepared composite nanomaterials with Au NPs supported on porous nitrogen-doped carbon (PNC) [86]. As effective electrocatalysts, these materials exhibited excellent HER performance. Excited by a 532 nm-wavelength light source, Au NPs exhibited LSPR-induced generation of thermal electrons. These electrons were transferred to the PNC's HER active sites (nitrogen-doped sites), promoting the HER, and the overpotential at a current density of 10 mA/cm² decreased from 196 to 99 mV. The potential mechanism for the high activity of these NCs was attributed to the synergy between the hot electrons exhibiting the LSPR-induced effect of Au NPs and the highly conductive PNC. This increased the thermal electrons' density of the electrocatalyst and enhanced the rapid transport of electrons. This study demonstrated broad application prospects for both energy conversion and photocatalysis, paving the way for the development of various catalytic reactions. At the same time, the LSPR effect is also extremely sensitive to the surrounding medium, which prompts future research on chemical sensors and biosensors based on optical signals. Regarding the plasmon SERS effect, as early as 1974, Fleischmann first discovered that pyridine on a rough Ag film can yield enhanced Raman spectroscopy. Three years later, the SERS effect was demonstrated, with

the potential of greatly enhancing the Raman signal of molecules near metal nanostructures. Since then, the SERS effect has garnered significant attention. Mei et al. developed novel three-dimensional Au@Ag NPs [87]. Compared with conventional Au@Ag NPs with smooth Ag shells, these novel NPs were based on Au NPs at the core, and Au NR arrays were grown vertically. The thiol ligand selectively blocked the surface and controlled the anisotropic growth of Ag NPs at the tip of Au NRs, thereby producing high-density homopolymerization (Ag-Ag) and heterogeneous (Au-Ag) hot spots in a single NP. These 3D hotspots increased the SERS effect of 3D Au@Ag NPs 30-fold, compared with the SERS effect of conventional Au@Ag NPs, enabling single-NP-level signal detection. This P-NM exhibits good optical properties and has been successfully applied in the fields of in vivo imaging and quantitative analysis of pollutants. The above examples show that the optical performance and high-efficiency optical and electrocatalytic performance exhibited by P-NMs cannot be ignored. The successful use of these properties and their application to actual needs will bring their advantages to the extreme.

Because P-NMs have excellent optical, magnetic, and mechanical properties [88-104], they have broad application prospects in the fields of energy storage devices, nanosensing technology, and medical treatment [45,105,106]. Although thermochemically induced photochemical synthesis materials have been increasingly reported in recent years, there are still only a few reports on plasmon-enhanced electrochemical catalysis and associated reactions. Moreover, at present, there is still little research on novel P-NM synthesis methods and their energy applications. Bo et al. proposed for the first time a novel solar radiation and postplasmon catalysis (SEPPC) process, in which toluene is effectively oxidized using a highly efficient and stable MnO2/graphenefinned foam (GFF) catalyst [107]. Using plasmon-enhanced chemical vapor deposition (CVD), GFF was synthesized as both a catalyst carrier and a light absorber. A modified MnO₂ nanofin on the GFF was used as a high-performance catalyst, yielding a fin-shaped MnO₂/GFF layer. In the SEPPC process, the energy efficiency of the toluene conversion was as high as 12.7 g kW/h, which was ~57% higher than for the postplasmon catalysis (PPC) process (8.1 g kW/h), which does not use solar radiation. In addition, the MnO₂/ GFF catalyst exhibited an excellent long-term catalytic stability, which was significantly better than that reported in earlier studies. This was mainly owing to the synergistic effect of the thermal effect of the solar hot surface and the MnO₂/GFF catalyst, which promoted the decomposition of ozone and enhanced the catalytic oxidation of the catalyst surface. Gellé et al. described the application of plasmon-enhanced nanocatalysis for organic conversion [108].

With regard to the applications of P-NMs, some earlier reviews summarized their applications to biosensing, environmental detection, and energy conversion [55,106,109-114]. Among these, the applications of P-NMs to energy have been very few. Devi and Kavitha summarized the surface metallization characteristics of plasmonic metal-TiO2 composite materials and their performance in energy and environmental applications [115]. Furube and Hashimoto elaborated on the latest advances in plasmonic thermal electron transport and plasmonic molecular drives, in both energy conversion and nanomanufacturing [116]. In addition, Subramanian et al. [117] and Ma et al. [106] reviewed the latest research on the electrocatalysis of plasmon-induced multicomponent nanostructured materials in fuel cell reactions and the nanostructure of plasmonic metal-semiconductor heterostructures. The potential use of materials in photocatalysis applications has been considered.

This review surveys various P-NMs and their synthesis methods that have been introduced recently. The existing applications of P-NMs in the energy field are also reviewed. In addition, the current challenges and future developments of P-NMs are summarized. The authors hope this review of the groundbreaking and extensive body of research will be of importance to researchers and will encourage the development of novel P-NMs, which in turn may help to expand their applicability.

2 Types of P-NMs

Metal-based P-NMs and carbon-based P-NMs are the two most common types of P-NMs. This article focuses on the synthesis methods of these two types of P-NMs. To compare the differences more conveniently, the synthetic method and application of metal-based P-NMs have been summarized in Table 1.

2.1 Metal-based P-NMs

Metal nanomaterials have important applications in the fields of biomedicine, sensory detection, surface-enhanced active bases, and environmental monitoring, owing to their SPR absorption characteristics. Noble metals themselves have a very high density of free electrons; therefore, plasmonic noble metal nanomaterials have always been of interest to researchers. However, the high cost of precious metals, the loss of light caused by the transition between energy bands and photons, and the shortage of Au and Ag

Table 1: Summary of metal-based P-NMs on synthetic method and application

Materials	Method	Application	Ref.
Au NRs	Reduction	Cancer cure	[118]
HAgNCs	Reduction	Photocatalysis	[119]
Co@Pt@Au	Reduction	Biosensing and therapeutics	[120]
Ag/ZnO	Reduction	Dye degradation	[121]
Au	Reduction	Pressure sensors	[122]
Bi-rGO/BiVO ₄	Reduction	Water splitting	[123]
MWO	One-pot	Sers substrate	[124]
$PB-MoO_{3-x}$	One-pot	Light stability	[125]
Fe ₃ O ₄ /TiN	One-pot	Photothermal conversion	[126]
CuS-PTX/SiO ₂	Template	Cancer therapy	[127]
Ag/TiO ₂	Template	Sensing	[128]
PRX-Ag	Template	Sequencing and detection	[129]
Au NPs	Seed-mediated	Data storage and printing	[130]
Au NRs	Seed-mediated	Diagnostics	[131]
Au NSs	Seed-mediated	Sensing	[132]
Au-beads@Ag	Seed-mediated	SERS and biomedical	[133]
Fe ₃ O ₄ @PEI-Au@PEI	Seed-mediated	SERS	[134]
Fe ₃ O ₄ @Au	Seed-mediated	Attomolar detection	[135]
AuNRs/MoS ₂	Seed-mediated	Combination therapy	[136]
Au@Pd NRs	Seed-mediated	Photocatalysis	[137]
Ag/rGO/TiO ₂	Chemical	PDSSC precipitation	[81]
Au	Electrochemical	Plasmonic biosensor	[138]
Au/Ag	Self-assembling	Cancer detection	[139]
AINTs-TiO ₂	Colloidal lithography	Ammonia production	[140]
MoO_{3-x}	Aqueous exfoliation	Energy storage	[141]
Noble metal/ZnO	Photothermal	SERS detection	[142]
Au	Reactive magnetron	Sensing	[143]
J-AgNP	Electrostatic adsorption	Colloidal stabilization	[144]
Ag-La/TiO ₂	Ultrasound-assisted wet	Photocatalysis	[145]
Au	Seedless and surfactant-free method	Neuroscience	[146]
Er ³⁺ /SiO ₂ /Au	Seed-mediated	Upconversion emission	[147]
Au@Ag NRs	Photothermal nanofurnace	Sers detection	[148]
Au-CS UCNPs	Sputtering and thermal annealing	Upconversion emission	[149]
Ag-La/TiO ₂ NPs	Wet impregnation method	Photocatalysis	[150]
Cu-CuO/TNTA	Electrochemical method	Photocatalysis	[151]

PDSSC: plasmonic dye-sensitized solar cells, TNTA: TiO_2 nanotube array, HAgNCs: hollow Ag nanocubes, and MWO: molybdenum tungsten oxide.

have caused researchers to devote increasing attention to the research of nonprecious metals. Among these, the key technology for preparing metal nanomaterials is the simultaneous control of the product size and morphology. To date, many methods for preparing metal nanomaterials have been developed; these can be divided into physical and chemical methods. The physical methods involve dispersing a block into small nanosized particles; this is typically achieved using ultrasound, electron sputtering, or gas phase approaches. The chemical methods use a metal compound as raw material, use a chemical reaction for generating NPs, and control the growth of these particles when forming metal NPs, for maintaining them on the nanoscale. As shown in Table 1, metal-based P-NMs prepared

using different synthesis methods have different morphologies, properties, and differ in their applicability to a certain extent. In this article, we review metal-based P-NMs obtained using different synthesis methods, mainly the reduction, one-pot, template, and seed-mediated methods.

2.1.1 Reduction method

The reduction method is simple, easy to use, and is one of the most commonly used methods for synthesizing NPs. A typical synthesis process involves adding different reducing agents to a solution containing metal ions, and the metal ions are reduced to an aggregate of nanometer-sized NPs. The synthesis method of Turkevich is one of the representative synthesis methods for preparing NPs. P-NMs can also be synthesized using the reduction method, and the P-NMs synthesized using this approach exhibit better performance than general nanomaterials. Moreover, the P-NMs synthesized by the reduction method constitute a single precious metal, the P-NM. Huang et al. synthesized plasmonic Au NRs (Figure 3a) using the ascorbic acid (AA) reduction of the Au salt HAuCl₄ solution, using the reduction method [118]. In addition, a microfluidic device embedded with microstructures was designed for aligning with a laser and a dark-field microscope to observe the effects of light and heat on cells in real time. Dadhich et al. synthesized plasmonic hollow Ag nanocubes (HAgNCs; Figure 3b shows the high-resolution transmission electron microscopy [HRTEM] image) with spherical void spaces, using the reduction method [119]. The first step amounted to adding AgNO₃ and folic acid to Milli-Q water. Then, the pH was adjusted with NaOH. Finally, folic acid-capped Ag₂O nanospheres were formed for obtaining HAgNCs during the reduction of hydrazine hydrate (the entire synthesis process is shown in Figure 3c). In the synthesis phase, the folic acid played a unique role as a shape and structure-directing agent. The synthesized HAgNCs were shown to be good catalysts in the dark and sunlight conditions and were shown to degrade a model dye methyl

orange. It was found that HAgNC-630 had the best catalytic effect, and the catalytic efficiency in sunlight was 3.3-fold that of solid Ag nanospheres. To improve the performance of single-precious-metal P-NMs, researchers have attempted to dope other single metals based on P-NMs, to form composites with potentially better performance. It was found that most doped substances were metals, metal oxides, and composite films. Katagiri et al. synthesized P-NM Co@Pt@Au NPs, using the reduction method [120]. First, Co-Pt NPs were synthesized by octanol reduction. The resulting NPs were added to HAuCl₄ containing a solution of formaldehyde and 1-octadecene. Then, Au-coated Co-Pt NPs were collected using a magnet, and finally Co@Pt@Au NPs were obtained through ligand exchange synthetic plasmon. In the course of this experiment, the researchers designed and synthesized complex multicomponent NPs through an adjustable reduction reaction. According to the Co/Pt ratio, the distribution of Co and Pt in the NPs was precisely controlled, and a CS structure with Co as the core and Pt as the shell was formed, as shown in Figure 4a-d. The synthesized plasmonic Co@Pt@Au NPs have a great potential for development in transportation and sensing applications. Ziashahabi et al. synthesized a novel cohybrid Ag/ZnO plasmonic nanostructure using the reduction method. The nanostructure was synthesized from ZnO in water using the arc discharge method, and then synthesized by coupling it with Ag using the chemical

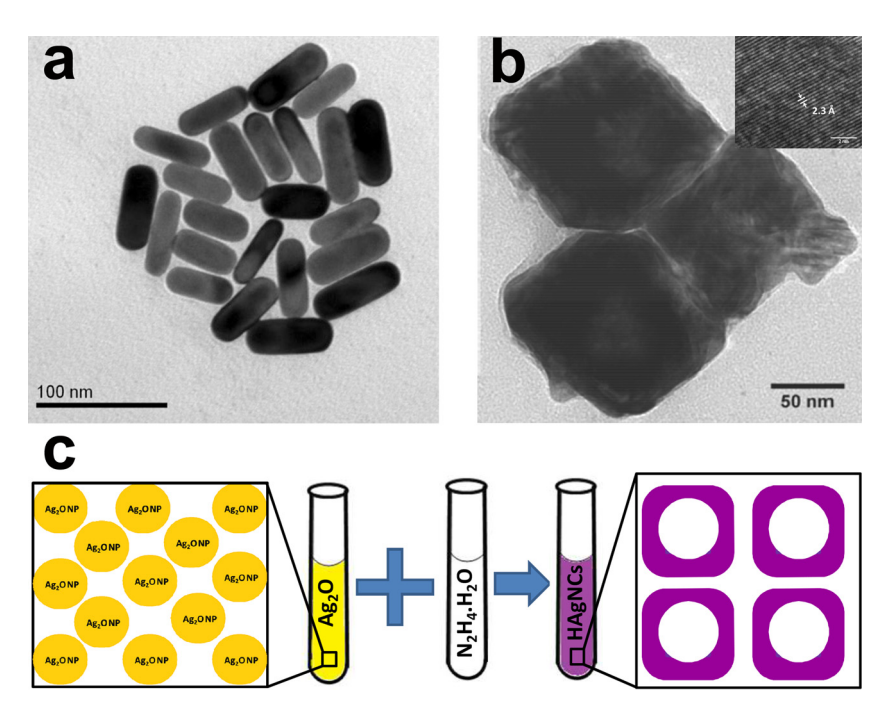


Figure 3: (a) Transmission electron microscopy (TEM) images of Au NRs, reproduced with permission [118]. Copyright 2019, Royal Society of Chemistry. (b) HRTEM image of HAgNC-630 and (c) synthesis scheme of HAgNCs, reproduced with permission [119]. Copyright 2018, American Chemical Society.

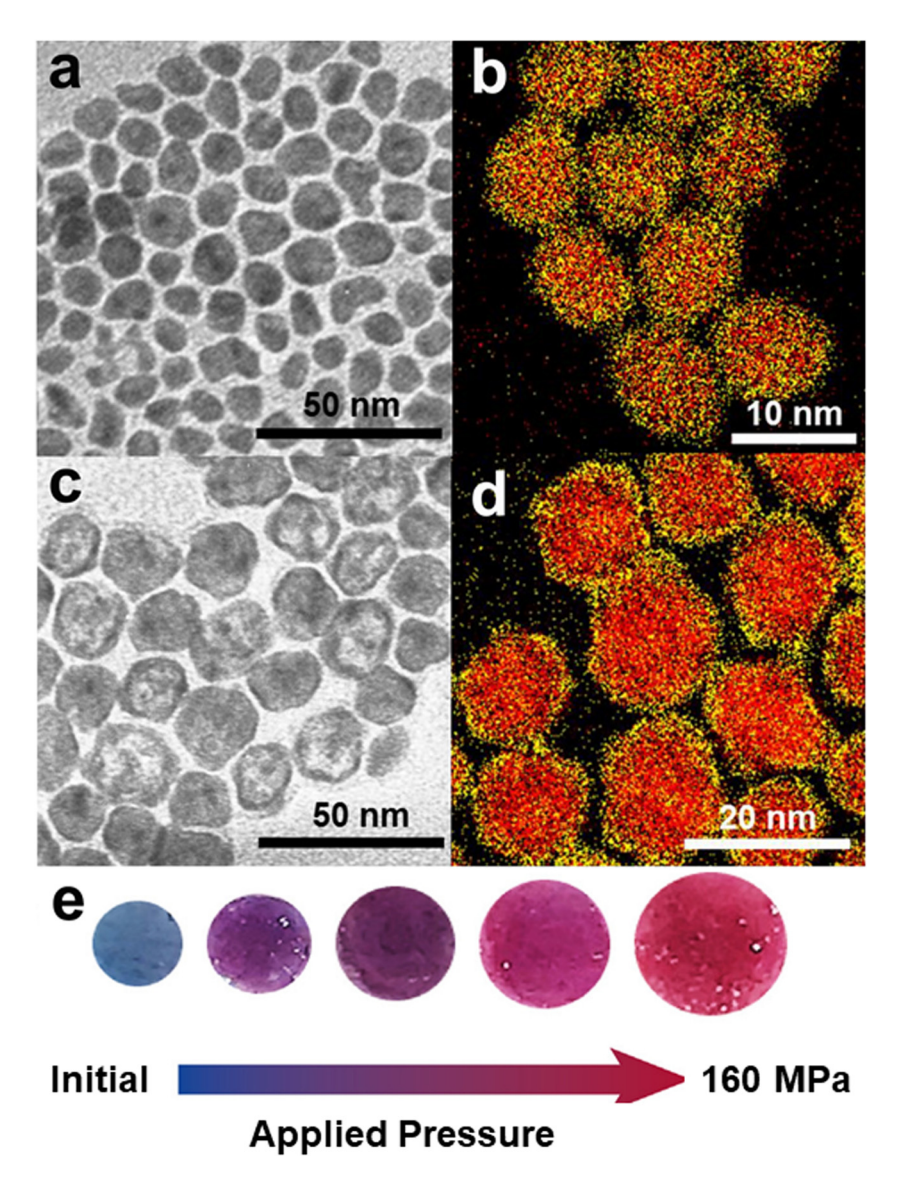


Figure 4: (a-d) TEM images and elemental spectra of Co-Pt NPs prepared with different Co/Pt precursor molar ratios; (a and b) Co:Pt = 60:40 and (c and d) Co:Pt = 70:30. Reproduced with permission [120]. Copyright 2020, American Chemical Society. (e) Appearance of the films used under various pressures. Reproduced with permission [123]. Copyright 2019, Elsevier.

reduction method [121]. The resulting structure induced the photocatalytic degradation of methylene blue under visible light and darkness conditions. Topcu *et al.* synthesized a plasmonic Au NP-embedded polyacrylamide (PAAm) composite membrane, using the reduction method [122]. First, HAuCl₄ was reduced with a trisodium citrate solution, for synthesizing Au NPs, after which a poly(vinylpyrrolidone) PVP solution and PAAm were added to the dispersion of Au NPs and left to dry in an oven, finally yielding the PAAm compound membrane. Through related characterization and research, it was found that the synthesized PAAm composite film is a self-supporting flexible polymer film with a strong optical response to mechanical pressure, as shown in

Figure 4e. Subramanyam *et al.* synthesized an rGO/BiVO₄ composite materials (Bi-rGO/BiVO₄) photoanode modified with plasmonic Bi NPs [123]. Bi NPs were synthesized using the chemical reduction method with sodium borohydride as a reducing agent, and the manufacturing of the photoelectrode was completed using the die-casting method. The composite electrode exhibited good light-hydrogen conversion efficiency, considerable incident photon-current efficiency, and low charge transfer resistance, and realized photoelectrochemical (PEC) water splitting. Benefited from the convenient operation, simple equipment, low investment, and good controllability, reduction method is widely used to obtain noble metal P-NMs. However, the biggest

limitation of reduction method is that it can only be used to prepare metals, especially noble metal, rather than metal oxides.

2.1.2 One-pot method

The one-pot method is simple, convenient, clean, and pollution-free and is one of the most widely considered synthesis methods. Li et al. synthesized surfactant-free plasmonic molybdenum tungsten oxide hybrid nano materials, using the one-pot method [124]. Substrates with excellent SERS performance are mainly limited to noble metals (Au and Ag), but it was shown that the synthesized materials could be used as high-performance substrates, with their SERS performance being equivalent to that of noble metals. The study offered novel SERS substrates based on nonnoble metals. Odda et al. also synthesized anoxic molybdenum oxide NP nanoagents (PB-MoO_{3-x} NCs) functionalized with Prussian blue (PB), using the one-pot synthesis method [125]. Thermal nanoagents were shown to be strongly therapeutic with respect to cancer cells, both in vivo and in vitro. Zeng and Xuan synthesized a photonic nanofluid composed of Janus-type magnetic plasmonic Fe₃O₄/TiN NPs, using the one-pot synthesis method, the characterization of which is shown in Figure 5a-c [126]. The prepared nanofluid exhibited a full spectral absorption

of incident sunlight. Those authors described a novel strategy that utilizes full-spectrum solar energy and controls the photothermal properties of nanofluids. One-pot method is one of the most widely considered synthesis methods because it can be used to conveniently and cleanly fabricate most kinds of nanomaterials. However, the conditional control in fabrication is still a major challenge for one-pot method.

2.1.3 Template method

The template method for synthesizing novel nanomaterials has been developed over the past 10 years. In general, we distinguish between the hard and soft template methods, based on their own characteristics and limitations. Soft templates come in many forms and, in general, are easy to construct. Yet, compared with hard templates, the stability of soft templates is poor; thus, the associated template efficiency is typically not sufficiently high. He *et al.* synthesized plasmonic CuS-PTX/SiO₂ composite nanocapsules using the soft template method of micelles [127]. This material exhibited unique colloidal stability, biocompatibility, high light-to-heat conversion efficiency, and NIR laser-stimulated drug release behavior and was judged to be very promising for NIR laser-driven collaborative chemical photothermal cancer treatment applications.

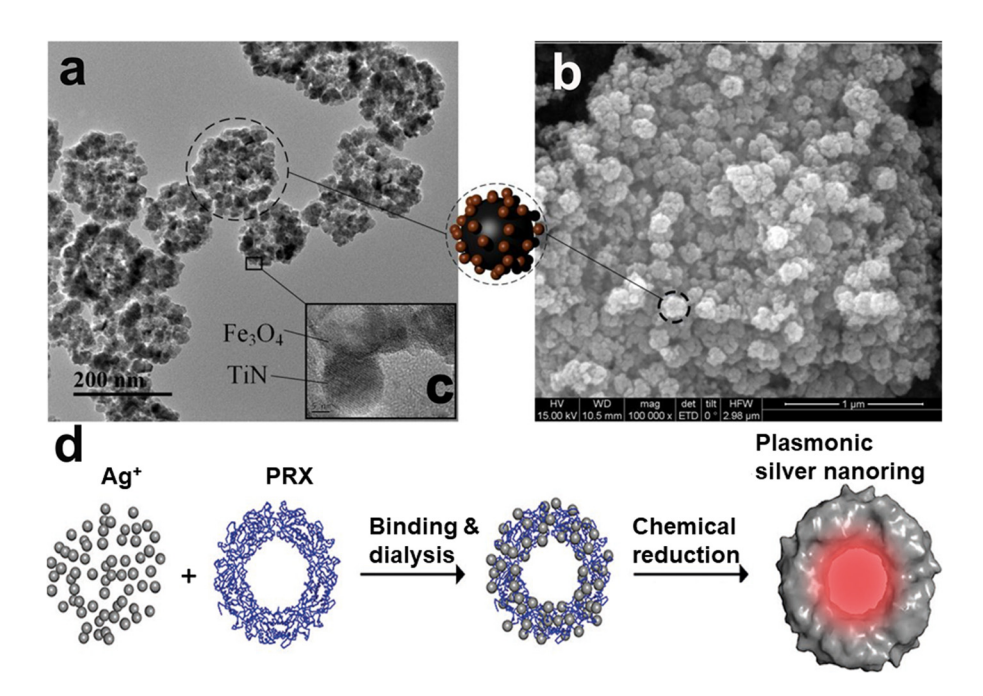


Figure 5: (a–c): (a) TEM, (b) SEM, and (c) HRTEM images of Fe₃O₄/TiN NPs (the dashed circle encircles a nanosphere), reproduced with permission [126]. Copyright 2018, Elsevier. (d) Synthesis flowchart of PRX–Ag NRs, reproduced with permission [129]. Copyright 2020, Wiley.

Guo et al. reported Ag⁺ ion-doped amorphous TiO₂ hollow spheres produced by etching a silica template and the following exchange of Ag⁺/Na⁺ ions [128]. The resultant material was used for formaldehyde detection. After exposure to increasing concentrations of formaldehyde, plasmonic Ag NPs were generated in situ, and photocurrent amplification was achieved in a proportional manner. This occurred owing to the injection of hot electrons from the plasmonic Ag NPs into the conduction band of amorphous titanium dioxide, which thereby enhanced the photocurrent. Giovannini et al. used peroxiredoxin (PRX) as a template for preparing nanopores, using a simple bioassisted method, and synthesized plasmonic Ag nanomaterials [129]. The spontaneous interaction between precious metals and biological scaffolds allowed to synthesize nanomaterials with unique characteristics that were simple and economical. PRX drove the growth of metallic Ag seeds under wet reduction conditions, and the inner and outer diameters of the generated nanorings were 28 and 3 nm, respectively, as shown in Figure 5d. Template method can more accurately control the size and morphology of nanomaterials than the other methods. However, the main challenges are how to obtain the suitable templates and how to get to remove templates without changing the original structure of nanomaterials.

2.1.4 Seed-mediated method

The particle size uniformity associated with the reduction method is not satisfactory. Compared with the reduction method, the seed-mediated method allows to control the size, shape, composition, and structure of the obtained nanocrystals. Cho et al. synthesized plasmonic chiral Au NPs using a multistep seed-mediated method [130]. The researchers divided the traditional sequence of singlechiral growth steps into two growth stages. First, chiral seed NPs were controllably synthesized from octahedral seed NPs, following which the helicoid was grown uniformly from the synthesized chiral seed NPs. They found that this multichiral evolutionary synthesis method can be applied to the morphology control of water-based nanocrystals, the synthesis of complex nanostructures such as chiral nanomaterials, and the synthesis of plasmonic metamaterials, with high uniformity and repeatability. Similarly, Li et al. used cetyltrimethylammonium bromide (CTAB) as a surfactant and an AA solution as a reducing agent and prepared plasmonic Au NRs using the seed-mediated method [131]. For wavelengths in the 300–700 nm range, by varying the irradiation time, it can be clearly seen from the spectrogram and the TEM image

in Figure 6a-c that the obtained Au NRs were gradually oxidized by light into Au particles. The researchers demonstrated the conversion between the photoreduction of Au ions and the photooxidation of Au NRs by varying the wavelength and also demonstrated that the seedmediated method can not only modulate the color of plasmon resonance in a contactless manner but can also modulate all-optical molding of individual NPs, providing a novel direction for reversibly adjusting the LPR effect. Liu et al. also used the seed-mediated method for synthesizing plasmonic Au nanostars (Au NSs) [132]. First, HAuCl₄ was used as a raw material, and sodium citrate was used as a reducing agent for reducing Au³⁺ into Au seeds; these Au seeds were then added to the PVP and mixed thoroughly to obtain Au NSs. Moreover, in the course of the study, a nanosensor was prepared using a plasmon and the photothermal immunoassay method, in which an enzyme triggered the crystal growth on Au NSs. The sensor detected low levels of alkaline phosphatase and easily read the test by color and temperature. Singh et al. prepared five-twin Au nanobeads by thermally induced seed twin synthesis, followed by the addition of AgNO₃ under magnetic stirring to grow Au-beads@Ag rods, and then converted them into plasmon by current displacement reaction (galvanic replacement reaction) Au nanocapsules [133]. Cetyltrimethylammonium chloride was used as a stabilizer, and an excessive growth of Ag on Au beads produced uniform Au beads@Ag NRs. The volume of AgNO3 added could be controlled for synthesizing Au-beads@Ag rods of different sizes (Figure 6d and e). In addition, this study also demonstrated that the hollow and porous CS nanostructures inherent in nanocapsules are of great significance in the field of SERS.

In addition to single-metal P-NMs, many researchers have explored single-metal P-NM derivatives, metal oxide P-NMs, and their derivatives. For single-metal P-NM derivatives, the most common derivative is based on singlemetal P-NMs doped with metals or metal oxides. Because the performance of a single-metal oxide P-NM is not very good, the research on metal oxide P-NMs basically addresses the composites of metal oxide P-NMs. The composite materials added on the basis of metal oxide P-NMs mainly consist of precious metals and polyelectrolytes. Pinheiro et al. successfully prepared a magnetic plasmonic nanoadsorbent based on Fe₃O₄ and Au, using the seedmediated method, which was encapsulated in a positively charged polyelectrolyte (polyethyleneimine) (Fe₃O₄@PEI-Au@PEI; Figure 6f and g) [134]. An aqueous solution containing AA and sodium citrate as reducing agents was used for reducing the Au salt to synthesize larger Au NPs (diameter, 70 nm). The final synthesized Fe₃O₄@PEI-Au@PEI was very promising for effective absorption/detection of 856 — Huiyu Duan et al. DE GRUYTER

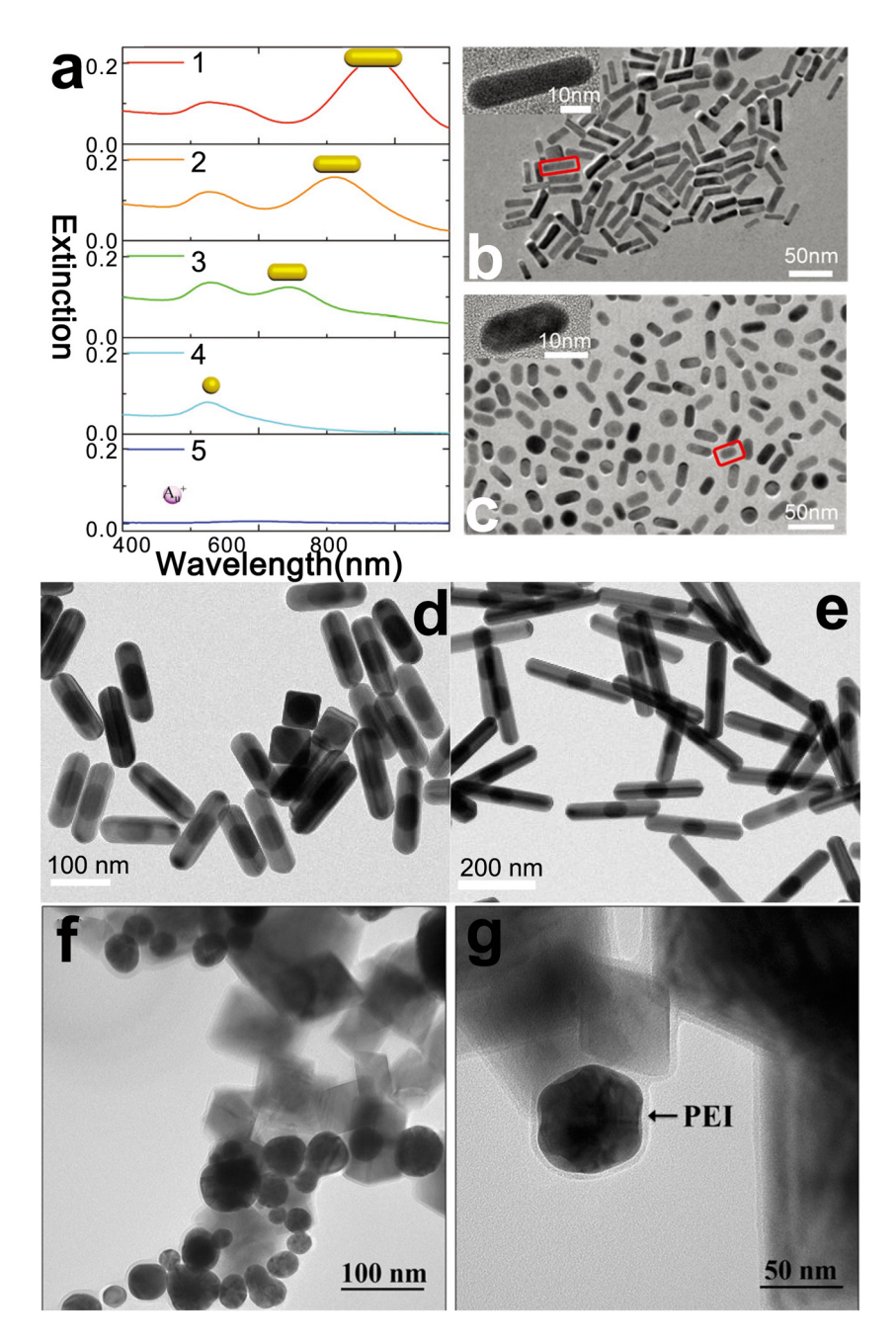


Figure 6: (a) Extinction spectra acquired for increasing irradiation times (0 min for curve 1, 90 min for curve 2, and 180 min for curve 3). (b) TEM images of the Au NRs were taken before oxidation and (c) after 180-min-long oxidation. The scale bars in the insets of (b) and (c) are 10 nm. Reproduced with permission [131]. Copyright 2018, Royal Society of Chemistry. (d and e) TEM image of an Au-bead@Ag NR. (d) Aspect ratio: 2.8 ± 0.2 . (e) Aspect ratio: 6.0 ± 0.3 . Reproduced with permission [133]. Copyright 2018, American Chemical Society. (f and g) TEM images of Fe₃O₄@PEI-Au@PEI. Reproduced with permission [134]. Copyright 2019, Springer Nature.

tetracycline. Al Mubarak synthesized P-NM Fe_3O_4 @Au NPs, using the seed-mediated method [135]. The local Au NPs on the surface were bridged to the Au shell carrying the detection probe of Fe_3O_4 @Au core/shell NPs through double hybridization assembly to form an Au substrate, so that the molar detection of microRNA (miRNA)-155 in solution could be performed. The results indicated that plasmonic

sensor chip applications for measuring biological binding events are feasible. Runowski *et al.* synthesized luminescent plasmonic KY_3F_{10} : Yb^{3+} , Er^{3+} / SiO_2 /Au nanomaterials using the seed-mediated method [147]. The surface Au NRs were reshaped into nanospheres at an NIR wavelength of 980 nm, and the color exhibited by the nanomaterials was adjusted by the emission wavelength (yellow to red).

To further improve the synthesis methods and improve the performance of synthesized P-NMs, some researchers have proposed combined methods. Younis et al. prepared a dual plasmonic photothermal therapy (PTT) nanoagent Au nanorods/MoS₂ (AuNRs/MoS₂) by combining the seedmediated and hydrothermal synthesis methods [136]. First, an Au seed solution was prepared by reducing HAuCl4 with NaBH₄, and then PEGylated MoS₂ nanosheets were synthesized using the hydrothermal method. Then, the two were ultrasonically mixed to finally prepare Au NR-modified polvethylene glycol-MoS₂ nanostructures. Studies have shown that the resultant material could be activated by a single low-power laser, and the proposed simultaneous photodynamic/synergistic PTT effect strategy could effectively reduce the treatment time and achieve a high treatment index. Shahine et al. synthesized a CS bimetallic plasmonic nanostructure (Au@Pd NR) using a combination of the seed-mediated and deposition methods [137]. Au seeds were added to the growth solution consisting of a mixture of CTAB, HAuCl₄, and AgNO₃ to initiate the growth of Au NRs. Related studies have shown that the plasmon-enhanced nanoenzyme activity of this preciousmetal nanostructure can be used for oxidative stressrelated therapeutic applications, and the adjustable LSPR in the NIR range has other advantages. Similar to the template method, the seed-mediated method can induce the formation of the P-NMs with particular sizes. However, the source of suitable seeds limits the application of the seedmediated method.

2.1.5 Other methods

Synthetic methods, such as the solvothermal method, the deposition method, the self-assembly method, photolithography technology, and mechanical lift-off methods, have also been considered in recent years. The solvothermal method is simple, inexpensive, green, and environmentally friendly and has always been among the most widely used synthetic methods. However, only a few synthetic approaches have been presented for preparing P-NMs. Javed et al. synthesized an Ag/rGO/TiO2 ternary plasmonic NC using a simple solvothermal method, and the synthesized material was suggested as a photoanode for high-efficiency PDSSCs [81]. The deposition methods for synthesizing P-NMs mainly include the electrochemical and chemical deposition methods. Klinghammer et al. synthesized plasmonic Au nanotubes by electrochemically depositing Au on the nanosized pores of an AAO matrix. On this basis, NaOH was used for etching away the surrounding AAO matrix, leaving only Au nanowires. It was found that a large array (area, ~1 cm²) of Au

NRs, arranged vertically and densely packed, can be used for local confinement and amplification of external light signals for reliable biosensing. Shehata et al. synthesized plasmonic Au cerium oxide NPs using chemical precipitation technology; this material can be used as an optical sensing material for lead particles in aqueous media based on fluorescence quenching [138]. Self-assembly is a method to spontaneously polymerize nanostructures using different interactions between specific active groups present in nature. It is a method for preparing novel biologically and chemically developed functional materials. Compared with general synthetic methods. P-NMs synthesized using the self-assembly approach have a more stable structure and exhibit better performance. Li et al. synthesized this plasmon nanostructure by self-assembling Au nanospheres selectively onto hollow Au/Ag alloy nanocubes. They used miRNAs, which are both cancer biomarkers and direct self-assembly triggers, as a target [139]. Through strict nucleic acid hybridization of the miRNA target, Au nanospheres selectively self-assembled to exhibit an ideal interparticle distance (~2.3 nm). The best SERS signal transmission was achieved for hollow Au/Ag alloy nanocubes. Two synthesis methods, photolithography and mechanical lift-off, were proposed recently. Thangamuthu et al. fabricated large-area plasmonic aluminum nanotriangles (AlNTs) through efficient and scalable colloidal lithography [140]. Etman et al. introduced a simple aqueous exfoliation strategy [141]. This method uses two commercial molybdenum oxide precursors, MoO₂ and MoO₃, with different weight ratios, to produce a series of plasmonic MoO_{3-x} nanosheets (where x represents oxygen vacancies). It was found that this material can be used as a negative electrode material for lithiumion batteries. In addition, there are some less common synthesis methods, such as combustion, vacuum evaporation, and thermal dehumidification methods. Although these approaches have not been widely adopted for synthetic P-NMs, each of them has a certain research value. Pathak et al. synthesized noble metal-doped ZnO by combustion and studied the effects of different metals (Ag, Au, and Pd) on the physical properties and on the LSPR performance [142]. The results showed that the combustion technology is a unique method. No further heat treatment was required for synthesizing a nanocrystalline material with a large surface area in a synthetic form. Kong et al. synthesized a plasmonic Au nanoisland (NI) array by vacuum evaporation [152]. A thin film of Au NIs was prepared by evaporating a 5 nm-thick Au layer on precleaned glass and a silicon substrate in high vacuum, followed by annealing at temperatures in the 200-600°C range, in the presence of argon. Subsequently, Eu³⁺-doped polycrystalline NaYF4 particles were deposited on the Au NI thin

films. Under the plasmon heat and the catalytic effect of Au NIs, polycrystalline $NaYF_4$ quickly transformed into single-crystal Y_2O_3 (the conversion process is shown in Figure 7a). This novel approach yielded single-crystal transformations at very low temperatures. After laser irradiation, optimized nanocrystals with better crystallinity and stability were produced. Yoshino *et al.* used thermal dehumidification to condense a coated Au film into nanodots, which is a simple and low-cost method for manufacturing uniform metal nanodots [143]. They successfully manufactured an array of Au nanodots with diameters in the 100-520 nm range, which responded to infrared light and could be used in infrared plasmonic sensors.

To further improve the overall performance of P-NMs, researchers have developed and tested many novel methods. Cao *et al.* prepared Au@Ag NRs into fully alloyed plasmonic AuAg NRs using a photothermal nanofurnace (TEM images are shown in Figure 7b and c) [148]. It was found that a silica shell can be used as both a thermal insulation layer and a protective layer, thereby promoting the alloying process. In addition, AuAg NRs maintained anisotropic nanostructures well after alloying. Therefore, the prepared AuAg alloy NRs exhibited excellent SPR performance, excellent chemical

resistance, and chemical stability, which could be used for SERS detection in practical applications. Guo et al. fabricated Janus plasmonic Ag nanosheets (J-Ag NPs) with two chemically different surfaces, using different electrostatic adsorption methods [144]. This approach avoids corrosive chemicals and high temperatures that can degrade Ag NPs. J-Ag NPs demonstrated a great potential for stabilizing emulsions and forming layered interfacial nanostructures. This novel method can be used for designing P-NMs at liquid-liquid and solid-liquid interfaces for achieving colloidal stability. Joint methods have also been considered. Koneti et al. synthesized plasmonic Au NPs using the reactive magnetron sputtering and deposition methods [145]. First, a thin film composed of Au (Au–TiO₂) dispersed in TiO₂ was obtained by reactive magnetron sputtering. Then, the Au–TiO₂ film was deposited on a substrate using the electrochemical method, following which the sample was subjected to vacuum annealing at different temperatures, at 10⁻³ Pa, to obtain Au NPs formed by the diffusion of Au atoms in the entire matrix. The obtained material featured small-sized Au NPs in the deposited Au-TiO₂ thin film, resulting in a negligible LSPR response. Clarke et al. synthesized Au-CS upconversion NPs (UCNPs) by large-

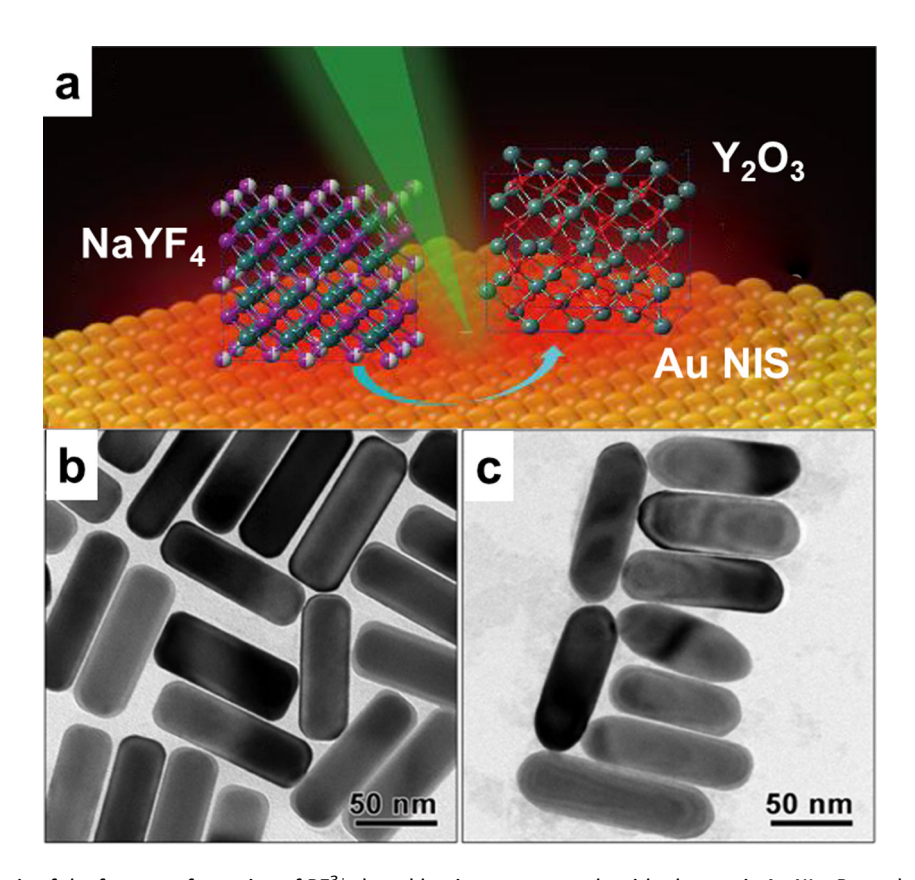


Figure 7: (a) Schematic of the fast transformation of RE³⁺-doped luminescent crystals with plasmonic Au NIs. Reproduced with permission [152]. Copyright 2020, Royal Society of Chemistry. (b and c) TEM images of original Au@Ag NRs-2.5 and fully alloyed AuAg NRs-2.5. Reproduced with permission [148]. Copyright 2018, American Chemical Society.

scale dewetting of plasmonic Au NPs onto CS UCNPs by sputtering and thermal annealing dehumidification [149]. The dehumidification method allows precise control of the shape and size of Au NPs over a wide range; thus, by adjusting their plasmon resonance to match the emission wavelength of the Er3+ emitter in NaYF4 UCNP17, the film thickness, annealing temperature, and annealing time can be simply changed. The design and integrated manufacturing methods of Au-CS-UCNPs provide a novel direction for exploring plasmon-enhanced upconversion emission. Dal'Toé et al. prepared lanthanum-doped titanium dioxide decorated with Ag plasmon NPs, using a simple green ultrasound-assisted wet impregnation method combined with photodeposition [150]. In addition, Sang et al. used TNTA photoanodes for synthesizing plasmonic Cu-CuO/TNTA in a two-step electrochemical method using environmentally friendly copper-based nanomaterials, followed by the sensitized synthesis with Eosin Y dye Eosin Y/Cu-CuO/TNTA [151]. This material enhances the transfer of interfacial charge and further increases the photocurrent density. In addition, the synthesis of most NIR-sensitive particles uses the seed-mediated synthesis method, but the surfactants used in the process (such as CTAB) are cytotoxic, and the process is complex. To resolve this problem, Lee et al. attempted to synthesize biocompatible plasmonic Au NSs using seedless and surfactant-free methods [146]. This method requires only biocompatible chemicals, 2-[4-(2hydroxyethyl)-1-piperazinyl] ethanesulfonic acid buffer and Au ions (HAuCl₄). The results demonstrated that the synthesized Au NSs can regulate nerves in response to the NIR irradiation.

2.2 Carbon-based P-NMs

When carbon-based nanomaterials are used as plasmonic materials, graphite and CNTs are the two most

commonly used carbon-based nanomaterials. Table 2 summarizes the carbon-based P-NMs on their synthetic method and application.

As early as 1958, researchers discovered that graphene has a layered structure (with a single-layer structure and a multilayer structure) and also learned that its layered structure originates from sp² bonded carbon atoms. In 2004, Novoselov et al. reported single-layer graphene prepared by mechanical peeling [153] and also demonstrated that graphene has good electrical conductivity, mechanical strength, thermal conductivity, and stability. As a result, graphene has garnered significant attention. Owing to the unique properties of graphene, an increasing number of studies have been conducted in recent years, considering it as a plasmonic material. Qiu et al. [160] adopted the idea of Chuntonov and Haran [161-163] and proposed a plasmonic trimer composed of graphene nanodisks. It was found that graphene nanostructures are more compact than general graphene structures and may have better applications in the optical field. Kanidi et al. [154] combined graphene and silicon to form a P-NM, which fully demonstrated the mechanical properties of graphene and the scalability of silicon. P-NMs were predicted to have good application prospects in disease diagnosis, sensing, and optics. Wang et al. synthesized GN@(y-FeO_x@AuNP)@ $[C_{60}(>DPAF-C_9)]_n$ P-NMs using the deposition method [155]. In addition, photo-induced changes in the relative dielectric properties of these materials were studied.

Owing to the controllability of the content and type of surface free radicals, GO and reduced graphene oxide (rGO) have been of increasing interest to researchers. Primo *et al.* synthesized GO-CHIT materials using a combination of an ultrasonic treatment and an amidation reaction [79]. Then, the obtained GO-CHIT was reduced with excess NaBH₄ to obtain the RGO-CHIT material. Then, GO, GO-CHIT and RGO-CHIT were characterized. Finally, the influence of the nature and number of graphene nanomaterials and the amount of immobilized

Table 2: Summary of carbon-based P-NMs on synthetic method and application

Materials	Method	Application	Ref.
Graphene	Mechanical peeling	Optical field	[153]
Graphene@silicon	Mechanical peeling	Disease diagnosis	[154]
$GN@[C_{60}(>DPAF-C_9)]_n$	Deposition	Biosensing	[155]
GO-CHIT	Ultrasonic treatment	Biosensing	[79]
AuAg@Au/RGO-C ₃ N ₄	Deposition	Photocatalysis	[156]
AuPLGA	Hummers	Disease treatment	[157]
CNTs	CVD	CO ₂ detection	[32]
eW-Au@CQDs	Chemical reduction	Methylene blue detection	[158]
CNTs	CVD	LSPR-based gas sensor	[159]

protein on the electrochemical and plasmonic properties of the relevant platform were clearly defined. Relatively speaking, GO has been the most studied graphene derivative as a P-NM. Wang et al. used the method of preparing Au@Ag (the synthesis process is shown in Figure 8a) [164]. Hou et al. synthesized Ag seeds, AuAg@Au, and RGO-C₃N₄ precursors [156]. On this basis, 10 µL RGO-C₃N₄ and 10 μL AuAg@Au were added dropwise to the electrode surface, and finally, the electrode modified with the AuAg@Au/RGO-C₃N₄ material was prepared. This study demonstrated that the AuAg@Au/RGO-C₃N₄ plasmonic material exhibits outstanding photoelectric properties. Chauhan et al. adopted the modified Hummers method for preparing hybrid plasmonic carbon nanomaterials, which are Au polylactic-co-glycolic acid (AuPLGA) NS-decorated graphene oxide nanosheets and IR780 loaded GO nanosheets [157]. Research has shown that they are very promising for disease treatment.

Laser ablation, arc discharge, and CVD are the main methods used for preparing CNTs [32]. When CNTs are used as P-NMs, they are mostly used in the field of sensing. Allsop *et al.* used the changes in the optical properties of CNTs to prepare an LSPR-based gas sensor for detecting gaseous CO_2 [159]. Cheung *et al.* found that the strong π -plasmon absorption of single-walled nanotubes (SWNTs) in the ultraviolet region is more sensitive to ion binding than absorption in the visible and NIR regions [165]. On this basis, they designed a special SWNT, which is an SWNT modified with carboxyl-terminated phospholipid-polyethylene glycol (PL-PEG-COOH; SWNT/PL-PEG-COOH).

Through scanning transmission electron microscopy (STEM), SEM, and AFM characterization (Figure 8b-d), a small bundle of SWNTs was demonstrated in the sample SWNT/PL-PEG-COOH. In sensing applications, it was found that the sample can be used for detecting Fe³⁺ metal ions. Therefore, researchers have proposed that when a specific binding chelating agent is attached to the surface of CNTs, it can be used for detecting specific metal ions. In addition, to improve the environment and to reduce the waste, Devi et al. attempted to extract useful substances from electronic waste products to produce carbon quantum dots (CODs) [158]. The study found that e-waste-derived CQDs (eW-CQDs) have good optical properties. In addition, the researchers also made eW-CQDs into plasmon nanostructures (eW-Au@CQDs) using a one-step chemical reduction strategy, in which eW-CQDs acted as reducing agents. At room temperature, a solution of 1 mM HAuCl4 and 0.3 M eW-CQD was continuously stirred at a ratio of 1:9 to prepare eW-Au@CQDs. After the reaction was completed, the solution was filtered through a syringe filter. Finally, the samples were stored at 4°C until further use.

2.3 Other materials

In addition to metal-based P-NMs and carbon-based P-NMs, there are other types of P-NMs, such as sulfur-based P-NMs and plasmon-active nanostructured films. Owing to the

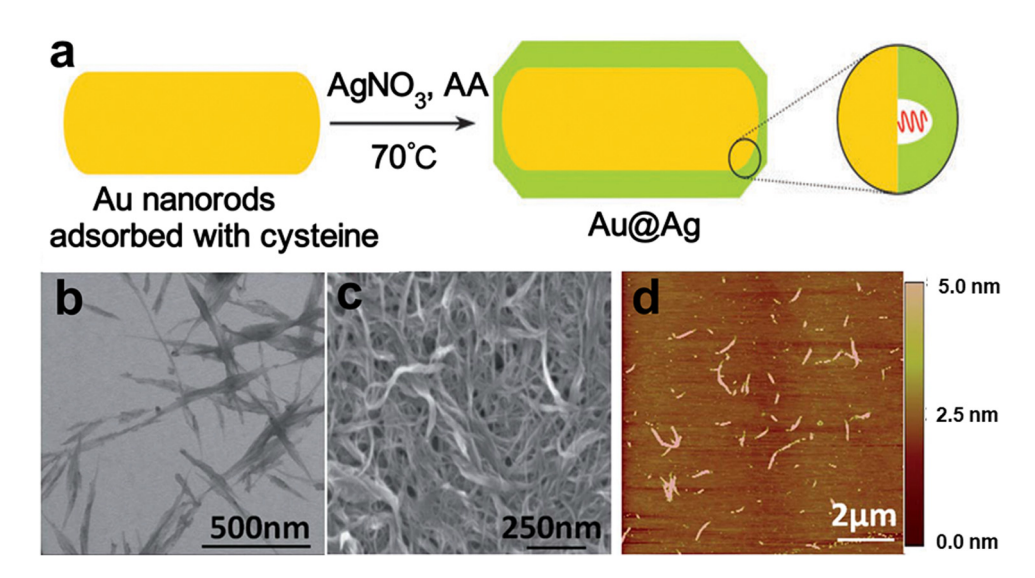


Figure 8: (a) Schematic of the preparation method. (b-d) STEM, SEM, and atomic force microscopy (AFM) images of SWNT/PL-PEG-COOHs, respectively. Reproduced with permission [164]. Copyright 2016, Springer Nature. (b-d) STEM, SEM, and AFM images of SWNT/PL-PEG-COOHs, respectively. Reproduced with permission [165]. Copyright 2016, Royal Society of Chemistry.

uniqueness of sulfur in nature, structure, and function, sulfur-based P-NMs have very good application prospects in mesoscopic physics and in the manufacturing of nanoscale devices. However, poor conductivity is a major problem with sulfur-based materials. At present, the best way to overcome this problem is to dope on this basis with good-conductivity materials, such as carbon, metals, and conductive polymers. In this regard, Teng et al. summarized and discussed the current research and challenges of sulfur-based materials and their plasmonic applications. Compared with general P-NMs, the preparation of plasmonics-active nanostructured thin films (PANTFs) on solid substrates has better physical stability. Among them, the SiO₂ substrate is the most widely used substrate for preparing PANTFs, owing to its advantages of low cost and easy preparation. In addition, excellent flexibility makes polymethyl methacrylate, polyethylene terephthalate, and polycarbonate polymers the most commonly used polymer substrates for creating PANTFs. To this end, Bhattarai et al. summarized the synthesis of PANTFs and outlined their sensitivity to biosensing [64].

3 Properties of P-NMs

In the continuing exploration and research of P-NMs, researchers have found that the P-NMs themselves have many excellent properties, including optical, magnetic, and other properties. Among these, the optical properties of P-NMs are the most prominent. Owing to these excellent properties, P-NMs can be widely used in various fields. In what follows, we review the main features of P-NMs.

3.1 Optical properties

Among all of the properties of P-NMs, optical properties are the most important for many applications; therefore, there is a need to optimize these properties for widening the usage scope of P-NMs. In contrast, improving the optical properties of these materials may help to further expand their application market; however, P-NMs can also be added to other materials, to improve the optical properties of resultant materials. Shahine [166], Yang *et al.* [167], Clarke *et al.* [149], and others have studied methods for enhancing the optical properties of P-NMs. They coupled metal NPs to semiconductor nanostructures, and excitons and plasmons interacted to form a hybrid system. Owing to the plasmon-mediated emission

interaction on the metal surface, it can be used to adjust the characteristics of photoluminescent agents, such as enhancing or quenching light. The integration of NPs affects the absorption and photoluminescence properties of other nanomaterials, thereby adjusting the photocatalytic activity of the entire chemical system (the enhancement effect is shown in Figure 9a-d). Prusty et al. studied the unique structural characteristics of tunable NIR LSPR spectroscopy and high free-electron-density 2D nanomaterials, which provide attractive alternative energy conversion products for plasmon-based precious-metal-based nanostructures [168]. In the study of PPC by Odda et al., a simple size/morphology control method was adopted. The prepared PB-MoO_{3-x} NC featured uniform-size particles (size, ~90 nm), had high water dispersibility, and strong light absorption in the first biological window [125]. This intense light absorption was caused by the plasmon resonance in the oxygen-deficient MoO_{3-x} semiconductor. In addition to luminescent agents, P-NMs can also act as photocatalysts. Cho et al. used the photocatalytic properties of P-NMs to dominate the photocatalytic disinfection process of Escherichia coli and enhance the chirality of chiral reactions [123,130]. When P-NMs are used as photocatalysts, they can also be applied to the energy field, in addition to the medical field. In terms of the solar energy utilization, the PEC effect of P-NMs can improve the absorption of radiation, enhance the quantum confinement effect and photosensitivity effect, and increase the conversion efficiency of the solar energy to hydrogen, or for preparing materials for the solar energy conversion. Metal-based P-NMs are the most commonly used P-NM photocatalyst materials. The SPR effect of metal-based P-NMs (such as Au, Ag, and Al) can improve the light absorption characteristics of organic photovoltaic cells (OPVs) and has been widely used. By introducing different metal nanostructures between adjacent layers of the active layer, buffer layer, electrode, or OPVs, multiple plasmon mechanisms have been demonstrated [144]. In a study by Thangamuthu et al., plasmonic AlNTs were used for studying the effect of plasmon on the production of photocatalytic ammonia [140]. Through electrochemical photocurrent measurements, the problem of plasmonic near-field coupling to semiconductors and AINT generating hot electrons was studied in detail. The results confirmed the successful production of ammonia by decomposing nitrogen at room temperature and atmospheric pressure. From the results obtained, it is clear that the use of a plasmonic aluminum structure can significantly increase the rate of ammonia production. In addition, when P-NMs are used as photocatalysts, they can decompose pesticides to alleviate environmental pollution. Studies have shown that P-NMs decomposed a typical organic pesticide, Pb-TiO₂,

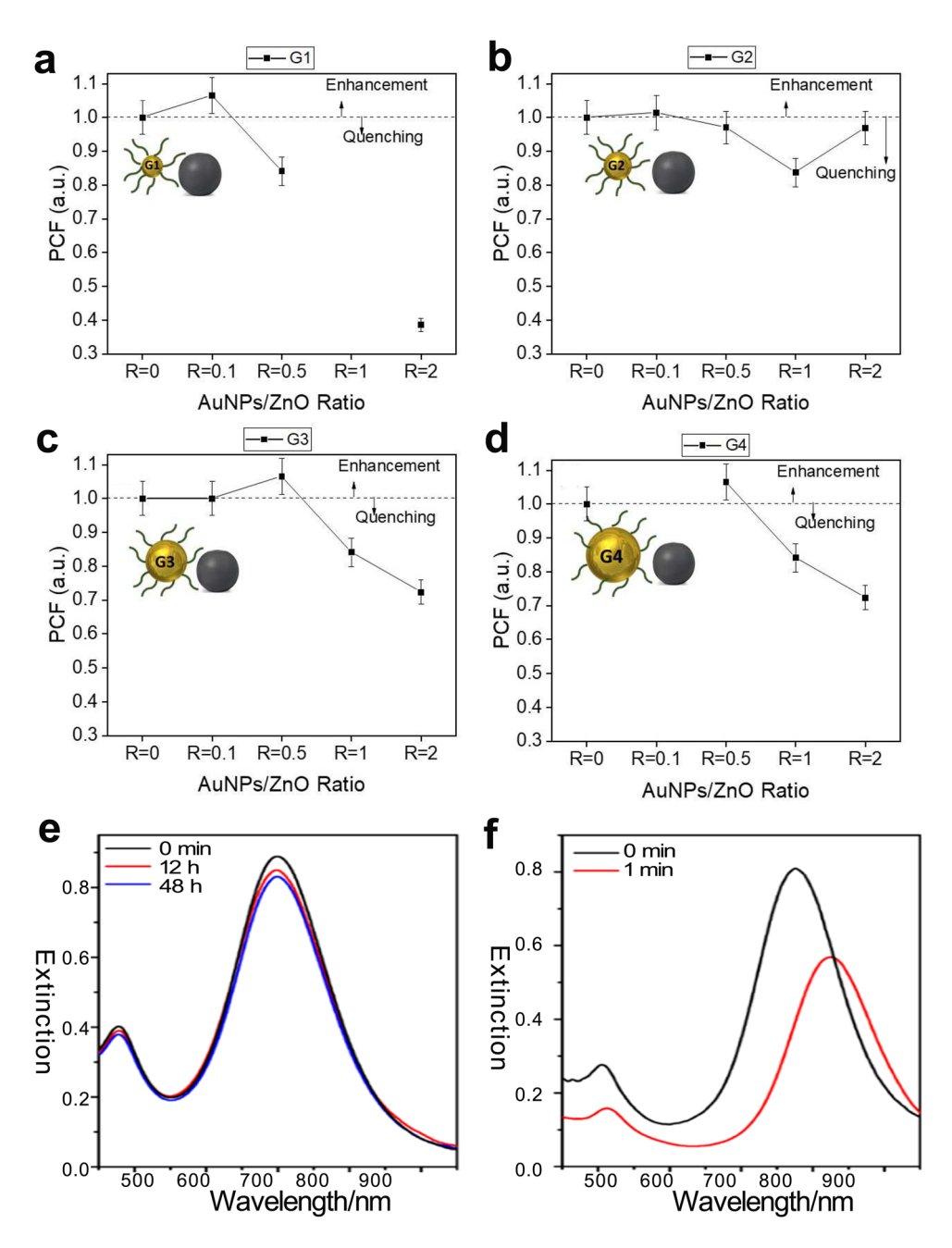


Figure 9: (a-d) Photocatalysis modification factor of hybrid samples, before (R = 0) and after the addition of various-size CTAB-capped Au NPs in different volumes into ZnONPs dispersions using (a) G1, (b) G2, (c) G3, and (d) G4. Reproduced with permission [137]. Copyright 2020, Wiley. (e and f) UV-vis extinction spectra showing the stability of (e) fully alloyed AuAg NRs-2.5 and (f) Au@Ag NRs-2.5 in a mixing solution of NH₄OH (0.5 M) and H₂O₂ (0.5 M). Reproduced with permission [148]. Copyright 2018, American Chemical Society.

when used as photocatalysts, and exhibited high photodegradation performance with respect to pesticides under 60 min of irradiation by sunlight [169]. In addition, P-NMs can also be used as key intermediates for constructing optical switches and tunable dielectric graphene nanomaterials and can be used for enhancing oxidase activity and cellular effects [170]. The above-mentioned extensive research shows that the optical properties of P-NMs have been widely used.

3.2 Magnetic properties

In addition to their optical properties, P-NMs also exhibit good magnetic properties. The magnetic properties of P-NMs can not only be used for synthesizing advanced nanomaterials but also for detection, diagnosis, and treatment of diseases in the medical field. Katagiri *et al.* designed CS NPs with excellent magnetic properties and

plasmon resonance: Co@Pt@AuNPs. First, Co@Pt NPs were synthesized using the ethanol reduction approach [120]. Then, Au was successfully coated on the Co@Pt NPs by uneven nucleation to form Co@Pt@Au NPs. Because Co@Pt NPs have excellent magnetic properties and a small lattice mismatch, the addition of Au coating increased the plasmon resonance effect, so Co@Pt@Au NPs exhibited excellent magnetic properties and plasmonic body response. These high-loudness hybrid nanosilicon graphene materials will greatly benefit from optoelectronic devices. Laser-structured plasmonic silicon is easy to manufacture, and its scalability, excellent electromagnetic (EM) enhancement performance, and successful integration with graphene provide convenience for sensing, photonics, optoelectronics, and medical diagnosis applications.

3.3 Other properties

The properties of P-NMs include but are not limited to optical properties and magnetic properties. Other properties are likely to affect the application range of these materials as well. Here, we mainly discuss the mechanical properties and chemical stability of P-NMs, which is relevant for sensing applications.

Kanidi et al. transferred graphene to uncoated nanostructured silicon and nanostructured silicon with Au NPs, using a graphene transfer process, and integrated silicon nanoarrays with graphene using laser processing [154]. Compared with traditional deposition and lithography methods, this manufacturing approach relied on a onestep method, which is cost-effective, allows to quickly process silicon in water using lasers, and is suitable for large-scale manufacturing. Excellent mechanical properties of graphene, combined with a scalable three-dimensional (3D) plasmonic nanostructured silicon substrate, enhanced the EM radiation characteristics of the P-NM and the substances with which it interacted. In addition to its good mechanical properties, the obtained P-NM also exhibited very good chemical stability. Cao et al. synthesized fully alloyed AuAg NRs in a photothermal furnace [148]; these AuAg NRs could convert absorbed light into heat energy. The silica shell in the synthetized material served as both a thermal insulation layer and a protective layer, for promoting the alloying process. The synthesized AuAg NRs exhibited improved plasmonic properties derived from Ag and were chemically stable in a corrosive environment derived from Au. The experiment explored the chemical stability of the Au-Ag CS NRs and fully alloyed AuAg NRs. The UV-vis spectra showed that,

after the fully alloyed NRs were kept in a mixed solution for 48 h, they still maintained their good plasmonic performance, whereas the band intensity exhibited only a small drop (~6%; Figure 9e). The plasmon energy band of these Au@Ag NRs exhibited a rapid red shift, indicating that the Ag shell was etched (Figure 9f). Guo et al. fabricated J-Ag NPs with two chemically different surfaces, using different electrostatic adsorption methods [144]. J-Ag NPs showed great potential for stabilizing emulsions and forming layered nanostructures at the interface potential. This novel method can be used for designing P-NMs at liquid-liquid and solid-liquid interfaces, for achieving colloidal stability. Topcu et al. [122] studied pressure sensors containing P-NMs. Nanostructures based on Au NPs are promising, owing to their plasmonic properties. In this study, based on polyacrylamide (PAAm) and Au NPs, a self-supporting flexible polymer film with a strong optical response after mechanical stress was prepared. This proposed a simple red-green-blue space-based algorithm that can be used for smartphone-assisted detection of applied pressure.

4 Energy applications of P-NMs

With increasing environmental pollution, reduction in the availability of fossil fuels, and increasing demands for clean energy, attention has turned to using wind, tidal, solar, and electrical energy sources that can alleviate the above-mentioned issues. Moreover, electrocatalysts and photocatalysts have been playing key roles in energy applications. Appropriate photocatalysts and electrocatalysts contribute to the sustainable use of water and air, increase the utilization of visible light, and stimulate the potential of energy storage devices, such as batteries and superchargers.

When the size of metal particle is considerably smaller than the wavelength of incident light, confinement of surface plasmons in the metal particle occurs as localized SPs, which present resonance effect as LSPR if the oscillation frequency coincides with the frequency of incident photons. The intensity and frequency of LSPR highly depend on the morphology, size, dispersion, composition, and the surrounding dielectric environment of the metal nanostructures. Benefited from EM fields near the surface of plasmonic metal nanostructures are greatly enhanced under LSPR excitation, light absorption could be distinctly boosted near the resonant frequency, which could competently meet the demands of solar-driven reactions. Besides, the intrinsic catalytic activity of metal nanostructures will also

contribute to the photocatalysis process. Through creation of energetic charge carriers and broadening of the absorption spectrum, these plasmonic metal nanostructures could effectively promote photocatalytic performance in H_2 production, CO_2 reduction, and other photoredox reactions.

As early as 1972, TiO₂ semiconductors were developed, realizing the photolysis of water. To determine suitable photocatalysts, extensive research has been conducted, and many semiconductor Au photocatalysts, such as ZnO, SnO₂, ZrO₂, and CdS, have been put forward. However, many problems remain associated with the use of these semiconductor materials as photocatalysts. The main problems are the low quantum rate, low solar energy utilization rate, and unclear mechanism of heterogeneous photocatalytic reactions of these materials. Much effort has been made to overcome these problems. Attempted improvement methods fall into two categories: (1) increasing the absorption wavelength by doping and (2) adding electron capture agents for effectively separating photogenerated electrons and holes. Novel photocatalysts, P-NMs, have been proposed. Among them, composites of precious metals and semiconductor metals are the most commonly considered P-NM photocatalysts. LSPR is a characteristic of P-NMs, which can extend the absorption range of light into the visible range. Moreover, the plasmonic effect of P-NMs can enhance the collection of visible light, extend the lifetime of charge carriers, improve the connection between electron and hole pairs, and stimulate the potential of redox reactions.

Plasmonic Au/TiO2 NPs synthesized by Yuan et al. were demonstrated to have perfect heterogeneous interfaces [171]. Related characterizations have also been carried out, including using HRTEM, X-ray photoelectron spectroscopy, Fourier-transform infrared, and PEC tests. A linear scanning voltammetry test (scanning rate, 20 mV/s; light intensity, 110 mW/cm²; xenon lamp power, 150 W) was performed for comparing the photocatalytic activities of TiO₂ NPs and plasmonic Au/TiO₂ in response to the UV-vis light irradiation. Figure 10a and b clearly shows that plasmonic Au/TiO₂ NPs exhibit better photocatalytic activity and corrosion resistance than TiO₂ NPs. In addition, the photocatalytic activity of this P-NM was shown to depend on the distance between Au and TiO2. In addition to noble metal and semiconductor metal composite materials, nonnoble metal, semiconductor metal composite materials, and single-metal materials also have potential as P-NM photocatalysts. Sang et al. synthesized TiO₂ nanotube arrays decorated with plasmon Cu, using the electrodeposition approach [151]. Cu plasmons enhanced the collection of visible light and increased the photocurrent density. Dadhich et al. made a simple modification based on a previously proposed synthesis method for plasmon photocatalyst HAgNC. The catalytic efficiency of the finally synthesized HAgNC-630 in sunlight was 3.3-fold higher than that of solid Ag nanospheres [119].

The above review suggests that based on the photoelectric catalytic performance of P-NMs, they can be suitably used in energy applications. In fact, P-NMs not only serves as good photoelectric catalysts but can also be used as energy-storing materials. The plasmonic effect of precious-metal-based nanomaterials can be utilized in energy storage devices, such as solar cells and supercapacitors, for improving their performance. Yang et al. [167] doped plasmonic Au NPs based on CsPbBr₃ perov skite nanotubes and found that the LSPR effect of the plasmonic Au NPs significantly improved the optical performance of the CsPbBr₃ perovskite nanocubes. Therefore, hybridization of perovskite halides with P-NMs is promising for improving the performance of photovoltaic devices (such as solar cells and supercapacitors). Deng et al. successfully embedded synthesized Au@Ag@SiO2 NCs into a perovskite film of a perovskite solar cell (Figure 10c-f) [108]. Clearly, as Figure 10 shows, the original perovskite surface was not dense and was very rough. Following the embedding of Au@Ag@SiO2 NCs, the roughness and density of the perovskite surface significantly improved. Interestingly, with increasing the amount of Au@Ag@SiO2 NCs, the improvement of the perovskite surface became more obvious. These results clearly show that embedding of plasmonic metal NPs strongly enhances the absorption of induced light and carrier separation ability, thereby increasing the photocurrent density and improving the performance of perovskite solar cells. Javed et al. synthesized Ag/rGO/TiO₂ anode materials using solvothermal methods. Owing to the LSPR effect of these materials, the performance of plasmon dye-sensitized solar cells improved [81]. In addition to precious-metal-based P-NMs, nonprecious-metalbased P-NMs were also considered for energy applications. Smith et al. synthesized plasmonic aluminum NPs using the solution method and studied the plasmonic energy transfer kinetics [172]. It was found that the transient optical response of plasmonic aluminum NPs is mainly determined by the evolution of the scattering cross-section, compared with plasmonic precious-metal-based NPs. Interestingly, a dual interface model suggested that the natural oxide layer of these plasmonic aluminum NPs caused rapid heat transfer. Subramanyam et al. synthesized Bi-rGO/ BiVO₄ supported by plasmonic Bi NPs, and adapted them for anode applications and PEC water splitting [123]. Owing to the surface plasmon behavior of Bi NPs, the resultant composite electrodes exhibited excellent energy conversion

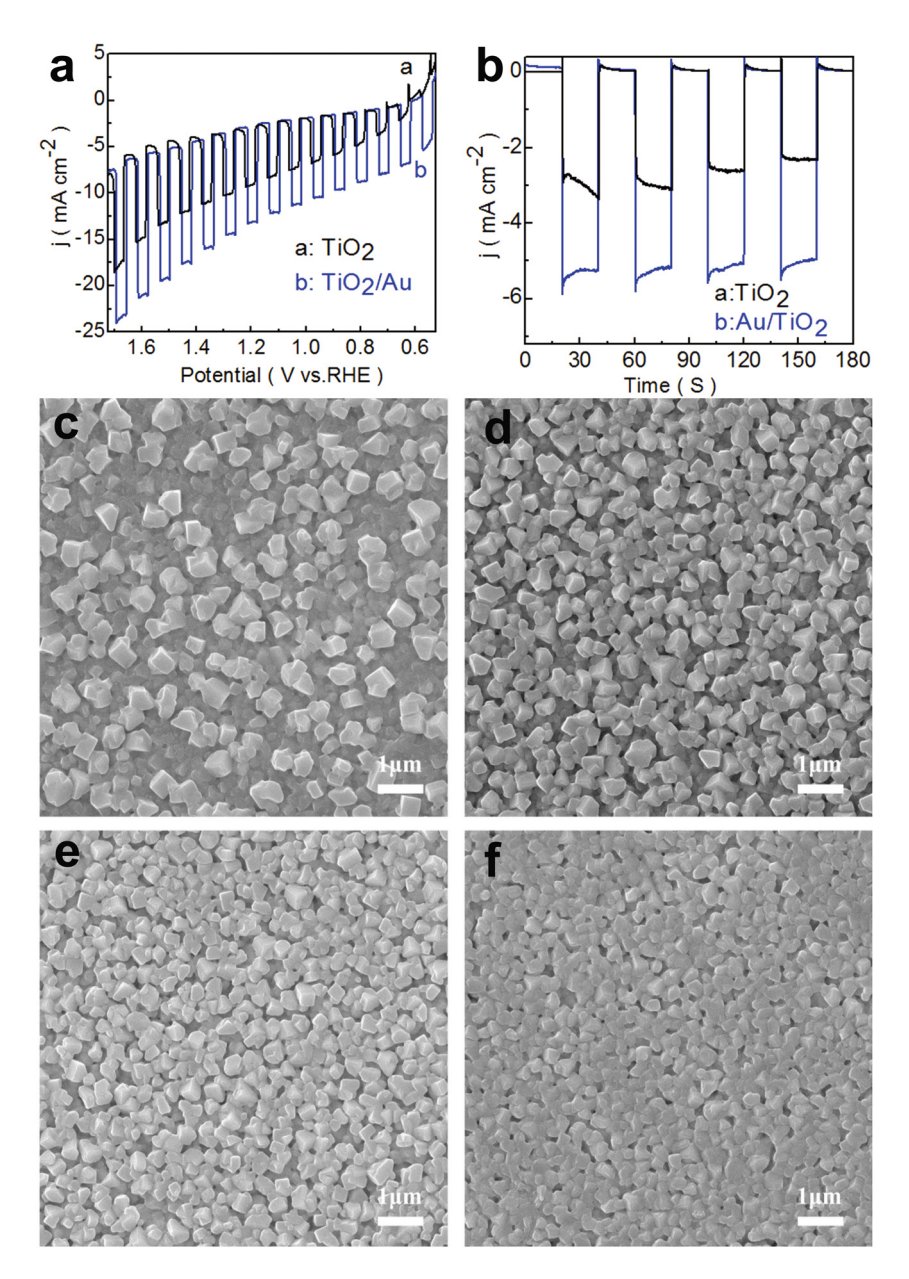


Figure 10: (a and b) Chopped illumination linear sweep voltammograms (a) and time domain photocurrents (b) of Au/TiO₂ NP-modified electrode in 0.1 M Na₂SO₄ aqueous solution, with pH adjusted to 11 by adding NaOH solution. Reproduced with permission [171]. Copyright 2018, American Chemical Society. (c-f) Top views of SEM images of a CH₃NH₃PbI₃ perovskite film (a) without and with (b) 0.5 vol%, (c) 1.0 vol%, and (d) 1.5 vol% Au@Ag@SiO₂ NCs addition. Reproduced with permission [108]. Copyright 2019, Elsevier.

efficiency, high current density, and low charge transfer resistance.

5 Conclusions and outlook

Compared with ordinary nanomaterials, P-NMs exhibit better performance and are very promising. Thus, in this article, we provided a brief overview of P-NMs. We summarized the relevant recent literature on metal-based P-NMs and carbon-based P-NMs. We showed that metal-based P-NMs exhibit excellent physical and chemical properties. In particular, their plasmon optical properties have garnered significant attention. Metal-based nanomaterials have important applications in the fields of biomedicine, sensory detection, surface-enhanced active bases, and environmental monitoring due to their SPR absorption characteristics. The first materials considered for metal-based P-NMs were the two precious metals, Au

and Ag. Noble metal-based materials have high density of free electrons; thus, plasmonic noble metal-based nanomaterials have been a research focus. However, precious metals also have disadvantages, such as low supply, high cost, and optical loss due to transitions between bands. Moreover, in subsequent research, it was found that nonprecious metal-based materials also have very good properties. Therefore, attention has been slowly switching to nonnoble-metal-based P-NMs. In addition, due to its good stability, electrical conductivity, mechanical strength, and thermal conductivity, carbon is becoming increasingly valuable for carbon-based P-NMs. The main types of considered carbon materials are graphene and CNTs.

For next-generation P-NMs, reduced production cost and increased scalability are equally crucial to ensure excellent energy storage and conversion performance. The construction of functional P-NMs can be controlled by simple methods. The main synthesis methods of P-NMs are the reduction, one-pot, template, seed-mediated, deposition, solvothermal, and self-assembly methods. We mainly reviewed the synthesis methods of metal-based P-NMs. These methods are heavily biased toward the reduction, one-pot, template, and seed-mediated methods. Both the reduction and one-pot methods have the advantages of simple synthesis and easy realization, but they also suffer from poor uniformity of the synthesized particles' sizes. The template method is a recently developed synthesis method and has the characteristics of diversity and easy construction. However, its template efficiency is not sufficiently high due to its poor stability; the seed-mediated method is relatively better. Seed-mediated method can provide amazing control over the size, shape, composition, and structure of nanocrystals.

Many effects have been discovered for P-NMs, such as the SPR effect, the LSPR effect, the SERS effect, the PRET effect, and the MO effect. Among these, the enhancement of the SERS and LSPR effects can significantly improve the performance of P-NMs. As a result, P-NMs exhibit excellent optical, magnetic, chemical, and mechanical properties. The present review focused on the optical and magnetic properties of P-NMs, and we discussed the utility of the optical properties for energy applications. When a synthesized NC material is excited by a light source, the formed plasmon thermal electrons can be transferred to the NC material, thereby increasing the number of catalytic active sites, potentially enhancing the charge density inside the material, and improving the electron transport speed, thus improving the material's photoelectric catalytic performance. Although the number of proposed thermochemically induced photochemical synthesis materials is constantly increasing, there are still only a few reports on plasmon-enhanced electrochemical catalysis and its reactions. Moreover, at present, there is still little research on the novel methods of synthesizing P-NMs and their energy applications. However, when P-NMs act as photoelectrocatalysts, the advantages of multiple catalytic active sites and faster electron transmission speed still have good market prospects in the energy field.

In summary, this review provides an introduction to the types and synthesis methods of P-NMs, the characteristics of P-NMs, and the energy applications of P-NMs. Although the materials have exhibited good performance. there is still a long way to achieve industrialization and commercialization of these materials. Cost is the fundamental problem to hinder industrialization and commercialization of these materials that complex synthesis is an important reason. We hope this review can provide an insight to identify new technique to determine the potential of P-NMs with different compositions and help researchers find easier approach to obtain these nanomaterials.

Funding information: This study was supported by the Key Projects of Basic Science (Natural Science) Research in Colleges and Universities of Jiangsu Province (21KJA150010): Program for the National Natural Science Foundation of China (Grant No. U1904215) and the Natural Science Foundation of Jiangsu Province (Grant No. BK20200044).

Author contributions: All authors have accepted responsibility for the entire content of this manuscript and approved its submission.

Conflict of interest: The authors state no conflict of interest.

References

- [1] Feng Q, Zhao S, Wang Y, Dong J, Chen W, He D, et al. Isolated single-atom Pd sites in intermetallic nanostructures: high catalytic selectivity for semihydrogenation of alkynes. J Am Chem Soc. 2017;139:7294-301. doi: 10.1021/ jacs.7b01471.
- [2] Wei Q, Xiong F, Tan S, Huang L, Lan EH, Dunn B, et al. Porous one-dimensional nanomaterials: design, fabrication and applications in electrochemical energy storage. Adv Mater. 2017;29:1602300. doi: 10.1002/adma.201602300.
- [3] Zhang F, Wei Y, Wu X, Jiang H, Wang W, Li H. Hollow zeolitic imidazolate framework nanospheres as highly efficient

- cooperative catalysts for [3 + 3] cycloaddition reactions. J Am Chem Soc. 2014;136:13963-6. doi: 10.1021/ja506372z.
- [4] Pang H, Zhang Y, Lai WY, Hu Z, Huang W. Lamellar K₂Co₃(P₂O₇)₂·2H₂O nanocrystal whiskers: High-performance flexible all-solid-state asymmetric micro-supercapacitors via inkjet printing. Nano Energy. 2015;15:303-12. doi: 10.1016/j.nanoen.2015.04.034.
- Zhu R, Ding J, Jin L, Pang H. Interpenetrated structures [5] appeared in supramolecular cages, MOFs, COFs. Coord Chem Rev. 2019;389:119-40. doi: 10.1016/j.ccr.2019.03.002.
- Zheng Y, Li X, Pi C, Song H, Gao B, Chu PK, et al. Recent advances of two-dimensional transition metal nitrides for energy storage and conversion applications. FlatChem. 2020;19:100149. doi: 10.1016/j.flatc.2019.100149.
- Hu W, Zheng M, Xu B, Wei Y, Zhu W, Li Q, et al. Design of [7] hollow carbon-based materials derived from metal-organic frameworks for electrocatalysis and electrochemical energy storage. J Mater Chem A. 2021;9:3880-917. doi: 10.1039/ d0ta10666f.
- [8] Du M, Li Q, Zhao Y, sen Liu C, Pang H. A review of electrochemical energy storage behaviors based on pristine metal-organic frameworks and their composites. Coord Chem Rev. 2020;416:213341. doi: 10.1016/j.ccr.2020.213341.
- [9] Wu S, Sun Y. An extreme-condition model for quantifying growth kinetics of colloidal metal nanoparticles. Nano Res. 2019;12:1339-45. doi: 10.1007/s12274-019-2297-8.
- [10] Wei Q, Guzman KG, Dai X, Attanayake NH, Strongin DR, Sun Y. Highly dispersed RuOOH nanoparticles on silica spheres: an efficient photothermal catalyst for selective aerobic oxidation of benzyl alcohol. Nano-Micro Lett. 2020;12:41. doi: 10.1007/s40820-020-0375-9.
- Sadeghi SM, Gutha RR. Ultralong phase-correlated networks of plasmonic nanoantennas coherently driven by photonic modes. Appl Mater Today. 2021;22:100932. doi: 10.1016/ j.apmt.2020.100932.
- [12] Wang C, Su Y, Tavasoli A, Sun W, Wang L, Ozin GA, et al. Recent advances in nanostructured catalysts for photoassisted dry reforming of methane. Mater Today Nano. 2021;14:100113. doi: 10.1016/j.mtnano.2021.100113.
- Zhang B, Huang J, Rutherford BX, Lu P, Misra S, Kalaswad M, et al. Tunable, room-temperature multiferroic Fe-BaTiO3 vertically aligned nanocomposites with perpendicular magnetic anisotropy. Mater Today Nano. 2020;11:100083. doi: 10.1016/j.mtnano.2020.100083.
- Rahman ST, Rhee KY, Park SJ. Nanostructured multifunctional electrocatalysts for efficient energy conversion systems: Recent perspectives. Nanotechnol Rev. 2021;10:137-57. doi: 10.1515/ntrev-2021-0008.
- [15] Bhat A, Budholiya S, Raj SA, Sultan MTH, Hui D, Shah AUM, et al. Review on nanocomposites based on aerospace applications. Nanotechnol Rev. 2021;10:237-53. doi: 10.1515/ntrev-2021-0018.
- Meng T, Ying K, Yang X, Hong Y. Comparative study on [16] mechanisms for improving mechanical properties and microstructure of cement paste modified by different types of nanomaterials. Nanotechnol Rev. 2021;10:370-84. doi: 10.1515/ntrev-2021-0027.
- [17] Sambandam B, Soundharrajan V, Kim S, Alfarugi MH, Jo J, Kim S, et al. K2V6O16-2.7H2O nanorod cathode: An advanced intercalation system for high energy aqueous rechargeable

- Zn-ion batteries. J Mater Chem A. 2018;6:15530-9. doi: 10.1039/c8ta02018c.
- [18] Soundharrajan V, Sambandam B, Kim S, Alfaruqi MH, Putro DY, Jo J, et al. $Na_2V_6O_{16}$ · $3H_2O$ barnesite nanorod: an open door to display a stable and high energy for aqueous rechargeable Zn-ion batteries as cathodes. Nano Lett. 2018;18:2402-10. doi: 10.1021/acs.nanolett.7b05403.
- [19] Liu J, Zhu D, Guo C, Vasileff A, Qiao S. Design strategies toward advanced MOF-derived electrocatalysts for energyconversion reactions. Adv Energy Mater. 2017;7:1700518. doi: 10.1002/aenm.201700518.
- [20] Lei Z, Xue Y, Chen W, Qiu W, Zhang Y, Horike S, et al. MOFsbased heterogeneous catalysts: new opportunities for energy-related CO2 conversion. Adv Energy Mater. 2018;8:1801587. doi: 10.1002/aenm.201801587.
- [21] Li X, Yang X, Xue H, Pang H, Xu Q. Metal-organic frameworks as a platform for clean energy applications. EnergyChem. 2020;2:100027. doi: 10.1016/j.enchem.2020.100027.
- Peng L, Fang Z, Zhu Y, Yan C, Yu G. Holey 2D nanomaterials for electrochemical energy storage. Adv Energy Mater. 2018;8:1702179. doi: 10.1002/aenm.201702179.
- Xu Q-T, Xue H-G, Guo S-P. FeS2 walnut-like microspheres [23] wrapped with rGO as anode material for high-capacity and long-cycle lithium-ion batteries. Electrochim Acta. 2018;292:1-9. doi: 10.1016/j.electacta.2018.09.135.
- [24] Duan H, Wang T, Wu X, Su Z, Zhuang J, Liu S, et al. CeO2 quantum dots doped Ni-Co hydroxide nanosheets for ultrahigh energy density asymmetric supercapacitors. Chin Chem Lett. 2020;31:2330-2. doi: 10.1016/j.cclet.2020.06.001.
- [25] Shan Y, Li Y, Pang H. Applications of tin sulfide-based materials in lithium-ion batteries and sodium-ion batteries. Adv Funct Mater. 2020;30:2001298. doi: 10.1002/ adfm.202001298.
- [26] Liu Y, Fu N, Zhang G, Xu M, Lu W, Zhou L, et al. Design of Hierarchical Ni-Co@Ni-Co layered double hydroxide coreshell structured nanotube array for high-performance flexible all-solid-state battery-type supercapacitors. Adv Funct Mater. 2017;27:1605307. doi: 10.1002/adfm.201605307.
- [27] Zhang W, Zhang F, Ming F, Alshareef HN. Sodium-ion battery anodes: Status and future trends. EnergyChem. 2019;1:100012. doi: 10.1016/j.enchem.2019.100012.
- [28] Wang G, Fu L, Zhao N, Yang L, Wu Y, Wu H. An aqueous rechargeable lithium battery with good cycling performance. Angew Chem - Int Ed. 2007;46:295-7. doi: 10.1002/ anie.200603699.
- [29] Wang F, Yu F, Wang X, Chang Z, Fu L, Zhu Y, et al. Aqueous Rechargeable Zinc/Aluminum Ion Battery with Good Cycling Performance. ACS Appl Mater Interfaces. 2016;8:9022-9. doi: 10.1021/acsami.5b06142.
- [30] Wu C, Gu S, Zhang Q, Bai Y, Li M, Yuan Y, et al. Electrochemically activated spinel manganese oxide for rechargeable aqueous aluminum battery. Nat Commun. 2019;10:73. doi: 10.1038/s41467-018-07980-7.
- He P, Yan M, Zhang G, Sun R, Chen L, An Q, et al. Layered VS₂ [31] nanosheet-based aqueous Zn ion battery cathode. Adv Energy Mater. 2017;7:1601920. doi: 10.1002/ aenm.201601920.
- [32] Eatemadi A, Daraee H, Karimkhanloo H, Kouhi M, Zarghami N, Akbarzadeh A, et al. Carbon nanotubes: properties, synthesis, purification, and medical applications.

- Nanoscale Res Lett. 2014;9:1-13. doi: 10.1186/1556-276X-
- [33] Nguyen TT, Mammeri F, Ammar S. Iron oxide and gold based magneto-plasmonic nanostructures for medical applications: a review. Nanomaterials. 2018;8:149. doi: 10.3390/ nano8030149.
- Chen Y, Chen Y, Chen G, Zheng X, He C, Feng S, et al. Discrimination of gastric cancer from normal by serum RNA based on surface-enhanced Raman spectroscopy (SERS) and multivariate analysis. Med Phys. 2012;39:5664-8. doi: 10.1118/1.4747269.
- Zangabad PS, Mirkiani S, Shahsavari S, Masoudi B, Masroor M, Hamed H, et al. Stimulus-responsive liposomes as smart nanoplatforms for drug delivery applications. Nanotechnol Rev. 2018;7:95-122. doi: 10.1515/ntrev-2017-0154.
- Ji M, Xu M, Zhang W, Yang Z, Huang L, Liu J, et al. Structurally well-defined Au@Cu2-xS core-shell nanocrystals for improved cancer treatment based on enhanced photothermal efficiency. Adv Mater. 2016;28:3094-101. doi: 10.1002/ adma.201503201.
- Xu M, Tu G, Ji M, Wan X, Liu J, Liu J, et al. Vacuum-tuned-[37] atmosphere induced assembly of Au@Ag core/shell nanocubes into multi-dimensional superstructures and the ultrasensitive IAPP proteins SERS detection. Nano Res. 2019;12:1375-9. doi: 10.1007/s12274-019-2325-8.
- Jeong GH, Sasikala SP, Yun T, Lee GY, Lee WJ, Kim SO. [38] Nanoscale assembly of 2D materials for energy and environmental applications. Adv Mater. 2020;1907006:1907006. doi: 10.1002/adma.201907006.
- [39] Simoncelli S, Li Y, Cortés E, Maier SA. Nanoscale control of molecular self-assembly induced by plasmonic hot-electron dynamics. ACS Nano. 2018;12:2184-92. doi: 10.1021/ acsnano.7b08563.
- [40] Liu J, Feng J, Gui J, Chen T, Xu M, Wang H, et al. Metal@semiconductor core-shell nanocrystals with atomically organized interfaces for efficient hot electron-mediated photocatalysis. Nano Energy. 2018;48:44-52. doi: 10.1016/ j.nanoen.2018.02.040.
- Wang H, Gao Y, Liu J, Li X, Ji M, Zhang E, et al. Efficient plasmonic Au/CdSe nanodumbbell for photoelectrochemical hydrogen generation beyond visible region. Adv Energy Mater. 2019;9:1803889. doi: 10.1002/aenm.201803889.
- Liu J, Pan R, Zhang E, Li Y, Xu M, Rong H, et al. Surface plasma resonance thermoelectric injection mechanism and research progress in photocatalysis and photocatalysis applications. Chin J Appl Chem. 2018;35:890-901.
- Feichtenschlager B, Pabisch S, Peterlik H, Kickelbick G. [43] Nanoparticle assemblies as probes for self-assembled monolayer characterization: correlation between surface functionalization and agglomeration behavior. Langmuir. 2012;28:741-50. doi: 10.1021/la2023067.
- [44] Pan M, Shi X, Lyu F, Levy-Wendt BL, Zheng X, Tang SKY. Encapsulation of single nanoparticle in fast-evaporating micro-droplets prevents particle agglomeration in nanocomposites. ACS Appl Mater Interfaces. 2017;9:26602-9. doi: 10.1021/acsami.7b07773.
- Zhou J, Yang T, Chen J, Wang C, Zhang H, Shao Y. Twodimensional nanomaterial-based plasmonic sensing applications: advances and challenges. Coord Chem Rev. 2020;410:213218. doi: 10.1016/j.ccr.2020.213218.

- Zhang J, Guan M, Lischner J, Meng S, Prezhdo OV. Coexistence of different charge-transfer mechanisms in the hot-carrier dynamics of hybrid plasmonic nanomaterials. Nano Lett. 2019;19:3187-93. doi: 10.1021/ acs.nanolett.9b00647.
- [47] Li W, He S, Xu W, Li J, Wang X. Synthesis of BiOCl-Ag/AgBr heterojunction and its photoelectrochemical and photocatalytic performance. Electrochim Acta. 2018;283:727-36. doi: 10.1016/j.electacta.2018.07.009.
- [48] Bonyár A. Label-free nucleic acid biosensing using nanomaterial-based localized surface plasmon resonance imaging: a review. ACS Appl Nano Mater. 2020;3:8506-21. doi: 10.1021/ acsanm.0c01457.
- [49] Zhou C, Zou H, Sun C, Ren D, Chen J, Li Y. Signal amplification strategies for DNA-based surface plasmon resonance biosensors. Biosens Bioelectron. 2018;117:678-89. doi: 10.1016/j.bios.2018.06.062.
- [50] Kari OK, Ndika J, Parkkila P, Louna A, Lajunen T, Puustinen A, et al. In situ analysis of liposome hard and soft protein corona structure and composition in a single label-free workflow. Nanoscale. 2020;12:1728-41. doi: 10.1039/ c9nr08186k.
- Jung I, Ih S, Yoo H, Hong S, Park S. Fourier transform surface [51] plasmon resonance of nanodisks embedded in magnetic nanorods. Nano Lett. 2018;18:1984-92. doi: 10.1021/ acs.nanolett.7b05439.
- [52] Zhao R, Wu Q, Tang D, Li W, Zhang X, Chen M, et al. Doubleshell CeO2:Yb, Er@SiO2@Ag upconversion composite nanofibers as an assistant layer enhanced near-infrared harvesting for dye-sensitized solar cells. J Alloy Compd. 2018;769:92-5. doi: 10.1016/j.jallcom.2018.07.225.
- [53] Souto DEP, Volpe J, de C, Gonçalves C, Ramos CHI, Kubota LT. A brief review on the strategy of developing SPR-based biosensors for application to the diagnosis of neglected tropical diseases. Talanta. 2019;205:120122. doi: 10.1016/ j.talanta.2019.120122.
- [54] Srivastava A, Verma A, Das R, Prajapati YK. A theoretical approach to improve the performance of SPR biosensor using MXene and black phosphorus. Optik. 2020;203:163430. doi: 10.1016/j.ijleo.2019.163430.
- Vivek C, Balraj B, Thangavel S. Electrical energy storage [55] capability of flake-like/spherical structured CuO-Ag nanocomposite synthesized by green plasmonic approach. J Electron Mater. 2020;49:1075-80. doi: 10.1007/s11664-019-07834-y.
- [56] Maurya J, François A, Prajapati Y. Two-dimensional layered nanomaterial-based one-dimensional photonic crystal refractive index sensor. Sensors. 2018;18:857. doi: 10.3390/ s18030857.
- [57] Ullah N, Mansha M, Khan I, Qurashi A. Nanomaterial-based optical chemical sensors for the detection of heavy metals in water: recent advances and challenges. TrAC Trends Anal Chem. 2018;100:155-66. doi: 10.1016/j.trac.2018.01.002.
- [58] Wang X, Shi W, Wang S, Zhao H, Lin J, Yang Z, et al. Twodimensional amorphous TiO2 nanosheets enabling highefficiency photoinduced charge transfer for excellent SERS activity. J Am Chem Soc. 2019;141:5856-62. doi: 10.1021/ jacs.9b00029.
- [59] Xue T, Liang W, Li Y, Sun Y, Xiang Y, Zhang Y, et al. Ultrasensitive detection of miRNA with an antimonene-based

- surface plasmon resonance sensor. Nat Commun. 2019;10:28. doi: 10.1038/s41467-018-07947-8.
- [60] Mahmoudpour M, Ezzati Nazhad Dolatabadi J, Torbati M, Pirpour Tazehkand A, Homayouni-Rad A, de la Guardia M. Nanomaterials and new biorecognition molecules based surface plasmon resonance biosensors for mycotoxin detection. Biosens Bioelectron. 2019;143:111603. doi: 10.1016/j.bios.2019.111603.
- Karimi-Maleh H, Kumar BG, Rajendran S, Qin J, Vadivel S, Durgalakshmi D, et al. Tuning of metal oxides photocatalytic performance using Ag nanoparticles integration. J Mol Liq. 2020;314:113588. doi: 10.1016/j.molliq.2020.113588.
- Kaushik S, Tiwari UK, Pal SS, Sinha RK. Rapid detection of Escherichia coli using fiber optic surface plasmon resonance immunosensor based on biofunctionalized Molybdenum disulfide (MoS 2) nanosheets. Biosens Bioelectron. 2019;126:501-9. doi: 10.1016/j.bios.2018.11.006.
- [63] Du J, Zhao M, Huang W, Deng Y, He Y. Visual colorimetric detection of tin(II) and nitrite using a molybdenum oxide nanomaterial-based three-input logic gate. Anal Bioanal Chem. 2018;410:4519-26. doi: 10.1007/ s00216-018-1109-4.
- Bhattarai JK, Uddin Maruf MH, Stine KJ. Plasmonic-active nanostructured thin films. Processes. 2020;8:1-20. doi: 10.3390/pr8010115.
- Gupta BD, Pathak A, Semwal V. Carbon-based nanomaterials [65] for plasmonic sensors: A review. Sens (Switz). 2019;19:3536. doi: 10.3390/s19163536.
- [66] Li X, Zhu J, Wei B. Hybrid nanostructures of metal/twodimensional nanomaterials for plasmon-enhanced applications. Chem Soc Rev. 2016;45:3145-87. doi: 10.1039/
- [67] Xie T, Jing C, Long YT. Single plasmonic nanoparticles as ultrasensitive sensors. Analyst. 2017;142:409-20. doi: 10.1039/c6an01852a.
- Bui QT, Yu IK, Gopalan AI, Saianand G, Kim W, Choi SH. Facile fabrication of metal oxide based catalytic electrodes by AC plasma deposition and electrochemical detection of hydrogen peroxide. Catalysts. 2019;9:888. doi: 10.3390/ catal9110888.
- [69] Ma S, Huang Y, Hong R, Lu X, Li J, Zheng Y. Enhancing photocatalytic activity of zno nanoparticles in a circulating fluidized bed with plasma jets. Catalysts. 2021;11:1-15. doi: 10.3390/catal11010077.
- Zhukeshov AM, Gabdullina AT, Amrenova AU, Fermakhan K. The pulse vacuum-arc plasma generator for nanoengineering application. Appl Phys A: Mater Sci Process. 2020;126:742. doi: 10.1007/s00339-020-03922-7.
- [71] Lee DY, Choi JH, Shin JC, Jung MK, Song SK, Suh JK, et al. Plasma functionalization of powdery nanomaterials using porous filter electrode and sample circulation. Appl Surf Sci. 2018;443:628-34. doi: 10.1016/j.apsusc.2018.02.194.
- Boyom-Tatchemo FW, Devred F, Ndiffo-Yemeli G, Laminsi S, Gaigneaux EM. Plasma-induced redox reactions synthesis of nanosized α -, γ - and δ -MnO2 catalysts for dye degradation. Appl Catal B: Environ. 2020;260:118159. doi: 10.1016/ j.apcatb.2019.118159.
- Smaglik N, Pokharel N, Ahrenkiel P. Applications of plasmaenhanced metalorganic chemical vapor deposition. J Cryst

- Growth. 2020;535:125544. doi: 10.1016/ j.jcrysgro.2020.125544.
- [74] el Sherbini AM, el Sherbini AE, Parigger CG. Measurement of electron density from stark-broadened spectral lines appearing in silver nanomaterial plasma. Atoms. 2018;6:44. doi: 10.3390/atoms6030044.
- Lee BJ, Shin DH, Lee S, Jeong GH. Revealing impact of plasma [75] condition on graphite nanostructures and effective charge doping of graphene. Carbon. 2017;123:174-85. doi: 10.1016/ j.carbon.2017.07.059.
- [76] Levchenko I, Xu S, Cherkun O, Baranov O, Bazaka K. Plasma meets metamatertials: three ways to advance space micropropulsion systems. Adv Physics: X. 2021;6:1834452. doi: 10.1080/23746149.2020.1834452.
- Jia P, Kong D, Ebendorff-Heidepriem H. Resist-free nanoim-[77] printing on optical fibers for plasmonic optrodes. Appl Mater Today. 2020;20:100751. doi: 10.1016/j.apmt.2020.100751.
- [78] Ma K, Li Y, Wang Z, Chen Y, Zhang X, Chen C, et al. Core-shell gold nanorod@layered double hydroxide nanomaterial with highly efficient photothermal conversion and its application in antibacterial and tumor therapy. ACS Appl Mater Interfaces. 2019;11:29630-40. doi: 10.1021/ acsami.9b10373.
- Primo EN, Bollo S, Rubianes MD, Rivas GA. Immobilization of [79] graphene-derived materials at gold surfaces: towards a rational design of protein-based platforms for electrochemical and plasmonic applications. Electrochim Acta. 2018;259:723-32. doi: 10.1016/j.electacta.2017.10.184.
- [80] Klinghammer S, Uhlig T, Patrovsky F, Böhm M, Schütt J, Pütz N, et al. Plasmonic biosensor based on vertical arrays of gold nanoantennas. ACS Sens. 2018;3:1392-400. doi: 10.1021/acssensors.8b00315.
- [81] Javed HMA, Qureshi AA, Salman Mustafa M, Que W, Shabir Mahr M, Shaheen A, et al. Advanced Ag/rGO/TiO2 ternary nanocomposite based photoanode approaches to highlyefficient plasmonic dye-sensitized solar cells. Opt Commun. 2019;453:124408. doi: 10.1016/j.optcom.2019.124408.
- [82] Lee SU, Jung H, Wi DH, Hong JW, Sung J, il Choi S, et al. Metalsemiconductor volk-shell heteronanostructures for plasmonenhanced photocatalytic hydrogen evolution. J Mater Chem A. 2018;6:4068-78. doi: 10.1039/c7ta09953c.
- [83] Scarabelli L, Hamon C, Liz-Marzán LM. Design and fabrication of plasmonic nanomaterials based on gold nanorod supercrystals. Chem Mater. 2017;29:15-25. doi: 10.1021/ acs.chemmater.6b02439.
- [84] Wang AX, Kong X. Review of recent progress of plasmonic materials and nano-structures for surface-enhanced Raman scattering. Materials. 2015;8:3024-52. doi: 10.3390/ ma8063024.
- [85] Jeong S, Kim MW, Jo YR, Kim NY, Kang D, Lee SY, et al. Hollow porous gold nanoshells with controlled nanojunctions for highly tunable plasmon resonances and intense field enhancements for surface-enhanced raman scattering. ACS Appl Mater Interfaces. 2019;11:44458-65. doi: 10.1021/ acsami.9b16983.
- [86] Zhang HX, Li Y, Li MY, Zhang H, Zhang J. Boosting electrocatalytic hydrogen evolution by plasmon-driven hot-electron excitation. Nanoscale. 2018;10:2236-41. doi: 10.1039/ c7nr08474a.

- [87] Mei R, Wang Y, Yu Q, Yin Y, Zhao R, Chen L. Gold nanorod array-bridged internal-standard SERS tags: from ultrasensitivity to multifunctionality. ACS Appl Mater Interfaces. 2020;12:2059-66. doi: 10.1021/acsami.9b18292.
- [88] Irum S, Jabeen N, Ahmad KS, Shafique S, Khan TF, Gul H, et al. Biogenic iron oxide nanoparticles enhance callogenesis and regeneration pattern of recalcitrant *Cicer arietinum L*. PLoS ONE. 2020;15:e0242829. doi: 10.1371/ journal.pone.0242829.
- [89] González-González RB, González LT, Iglesias-González S, González-González E, Martinez-Chapa SO, Madou M, et al. Characterization of chemically activated pyrolytic carbon black derived from waste tires as a candidate for nanomaterial precursor. Nanomaterials. 2020;10:1–22. doi: 10.3390/ nano10112213.
- [90] Pelclova D, Zdimal V, Komarc M, Schwarz J, Ondracek J, Ondrackova L, et al. Three-year study of markers of oxidative stress in exhaled breath condensate in workers producing nanocomposites, extended by plasma and urine analysis in last two years. Nanomaterials. 2020;10:1–25. doi: 10.3390/ nano10122440.
- [91] Yang W, Sun M, Song H, Su Y, Lv Y. A novel method to synthesize luminescent silicon carbide nanoparticles based on dielectric barrier discharge plasma. J Mater Chem C. 2020;8:16949-56. doi: 10.1039/d0tc04658b.
- [92] Liu J, Wu A, Tian R, Paredes Camacho RA, Zhou S, Huang H, et al. Progressive lithiation of FeP2 nanoparticles constrained inside the carbon shell. Mater Today Energy. 2020;18:100545. doi: 10.1016/j.mtener.2020.100545.
- [93] O'Connor D, Hou D, Liu Q, Palmer MR, Varma RS. Nature-inspired and sustainable synthesis of sulfur-bearing fe-rich nanoparticles. ACS Sustain Chem Eng. 2020;8:15791–808. doi: 10.1021/acssuschemeng.0c03401.
- [94] Fernández G, Pleixats R. Rhodium nanoparticles stabilized by peg-tagged imidazolium salts as recyclable catalysts for the hydrosilylation of internal alkynes and the reduction of nitroarenes. Catalysts. 2020;10:1–18. doi: 10.3390/ catal10101195.
- [95] Wang Z, Xia L, Chen J, Ji L, Zhou Y, Wang Y, et al. Fine characterization of natural SiO2-doped catalyst derived from mussel shell with potential photocatalytic performance for organic dyes. Catalysts. 2020;10:1–13. doi: 10.3390/catal10101130.
- [96] Ji T, Xu X, Wang X, Cao N, Han X, Wang M, et al. Background-free chromatographic detection of sepsis biomarker in clinical human serum through near-infrared to near-infrared upconversion immunolabeling. ACS Nano. 2020;14:16864-74. doi: 10.1021/acsnano.0c05700.
- [97] Liu M, Yu Q, Chen W, Liu X, Alvarez PJJ. Engineering of CoSe2 nanosheets via vacancy manipulation for efficient cancer therapy. ACS Appl Bio Mater. 2020;3:7800-9. doi: 10.1021/ acsabm.0c00981.
- [98] Yang J, Zhang Y, Guo J, Fang Y, Pang Z, He J. Nearly monodisperse copper selenide nanoparticles for recognition, enrichment, and sensing of mercury ions. ACS Appl Mater Interfaces. 2020;12:39118–26. doi: 10.1021/ acsami.0c09865.
- [99] Tao D, Gu Y, Song S, Nguyen EP, Cheng J, Yuan Q, et al. Ultrasensitive detection of alpha-synuclein oligomer using a PolyD-glucosamine/gold nanoparticle/carbon-based

- nanomaterials modified electrochemical immunosensor in human plasma. Microchemical J. 2020;158:105195. doi: 10.1016/j.microc.2020.105195.
- [100] Zeng G, Chen Y. Surface modification of black phosphorusbased nanomaterials in biomedical applications: Strategies and recent advances. Acta Biomaterialia. 2020;118:1–17. doi: 10.1016/j.actbio.2020.10.004.
- [101] Ahn HT, An HR, Hong YC, Lee SC, Le TN, Le XA, et al. Ultrarapid, size-controlled, high-crystalline plasmamediated synthesis of ceria nanoparticles for reagent-free colorimetric glucose test strips. Sens Actuators, B: Chem. 2020;320:128404. doi: 10.1016/j.snb.2020.128404.
- [102] Blokpoel Ferreras LA, Scott D, Vazquez Reina S, Roach P, Torres TE, Goya GF, et al. Enhanced cellular transduction of nanoparticles resistant to rapidly forming plasma protein coronas. Adv Biosyst. 2020;4:2000162. doi: 10.1002/ adbi.202000162.
- [103] Su C, Huang K, Li HH, Lu YG, Zheng DL. Antibacterial properties of functionalized gold nanoparticles and their application in oral biology. J Nanomaterials. 2020;2020:5616379. doi: 10.1155/2020/5616379.
- [104] Sapari S, Razak NHA, Hasbullah SA, Heng LY, Chong KF, Tan LL. A regenerable screen-printed voltammetric Hg(II) ion sensor based on tris-thiourea organic chelating ligand grafted graphene nanomaterial. J Electroanalytical Chem. 2020;878:114670. doi: 10.1016/j.jelechem.2020.114670.
- [105] Petrescu DS, Blum AS. Viral-based nanomaterials for plasmonic and photonic materials and devices. Wiley Interdiscip Reviews: Nanomed Nanobiotechnology. 2018;10:e1508. doi: 10.1002/wnan.1508.
- [106] Ma L, Chen S, Shao Y, Chen YL, Liu MX, Li HX, et al. Recent progress in constructing plasmonic metal/semiconductor hetero-nanostructures for improved photocatalysis. Catalysts. 2018;8:634. doi: 10.3390/catal8120634.
- [107] Bo Z, Yang S, Kong J, Zhu J, Wang Y, Yang H, et al. Solar-enhanced plasma-catalytic oxidation of toluene over a bifunctional graphene fin foam decorated with nanofin-like MnO2. ACS Catal. 2020;10:4420-32. doi: 10.1021/acscatal.9b04844.
- [108] Deng W, Yuan Z, Liu Z, Yang Z, Li J, Wang X, et al. Plasmonic enhancement for high-efficiency planar heterojunction perovskite solar cells. 2019;432:122–18. doi: 10.1016/ j.jpowsour.2019.05.067.
- [109] Takemura K, Adegoke O, Takahashi N, Kato T, Li TC, Kitamoto N, et al. Versatility of a localized surface plasmon resonance-based gold nanoparticle-alloyed quantum dot nanobiosensor for immunofluorescence detection of viruses. Biosens Bioelectron. 2017;89:998–1005. doi: 10.1016/j.bios.2016.10.045.
- [110] Sriram P, Manikandan A, Chuang FC, Chueh YL. Hybridizing plasmonic materials with 2D-transition metal dichalcogenides toward functional applications. Small. 2020;16:1–27. doi: 10.1002/smll.201904271.
- [111] Yoon J, Shin M, Lee T, Choi JW. Highly sensitive biosensors based on biomolecules and functional nanomaterials depending on the types of nanomaterials: a perspective review. Materials. 2020;13:1–21. doi: 10.3390/ma13020299.
- [112] Sriram M, Zong K, Vivekchand SRC, Justin Gooding J. Single nanoparticle plasmonic sensors. Sens (Switz). 2015;15:25774–92. doi: 10.3390/s151025774.

- [113] Tian Y, Zhang L, Wang L. DNA-functionalized plasmonic nanomaterials for optical biosensing. Biotechnol J. 2020;15:1-9. doi: 10.1002/biot.201800741.
- [114] Homaeigohar S, Elbahri M. Switchable plasmonic nanocomposites. Adv Optical Mater. 2019;7:1-33. doi: 10.1002/ adom.201801101.
- [115] Devi LG, Kavitha R. A review on plasmonic metal-TiO 2 composite for generation, trapping, storing and dynamic vectorial transfer of photogenerated electrons across the Schottky junction in a photocatalytic system. Appl Surf Sci. 2016;360:601-22. doi: 10.1016/j.apsusc.2015.11.016.
- [116] Furube A, Hashimoto S. Insight into plasmonic hot-electron transfer and plasmon molecular drive: new dimensions in energy conversion and nanofabrication. NPG Asia Mater. 2017;9:e454. doi: 10.1038/am.2017.191.
- [117] Subramanian P, Meziane D, Wojcieszak R, Dumeignil F, Boukherroub R, Szunerits S. Plasmon-induced electrocatalysis with multi-component nanostructures. Materials. 2018;12:1-12. doi: 10.3390/ma12010043.
- [118] Huang YC, Lei KF, Liaw JW, Tsai SW. The influence of laser intensity activated plasmonic gold nanoparticle-generated photothermal effects on cellular morphology and viability: A real-time, long-term tracking and monitoring system. Photochem Photobiolog Sci. 2019;18:1419-29. doi: 10.1039/ c9pp00054b.
- [119] Dadhich BK, Bhushan B, Saha A, Priyam A. Folate-directed shape-transformative synthesis of hollow silver nanocubes: plasmon tunability, growth kinetics, and catalytic applications. ACS Appl Nano Mater. 2018;1:4294-305. doi: 10.1021/acsanm.8b01110.
- [120] Katagiri M, Cuya Huaman JL, Matsumoto T, Suzuki K, Miyamura H, Balachandran J. Magneto-plasmonic Co@Pt@Au nanocrystals for biosensing and therapeutics. ACS Appl Nano Mater. 2020;3:418-27. doi: 10.1021/ acsanm.9b02040.
- [121] Ziashahabi A, Prato M, Dang Z, Poursalehi R, Naseri N. The effect of silver oxidation on the photocatalytic activity of Ag/ ZnO hybrid plasmonic/metal-oxide nanostructures under visible light and in the dark. Sci Rep. 2019;9:1-12. doi: 10.1038/s41598-019-48075-7.
- [122] Topcu G, Guner T, Inci E, Demir MM. Colorimetric and plasmonic pressure sensors based on polyacrylamide/Au nanoparticles. Sens Actuators, A: Phys. 2019;295:503-11. doi: 10.1016/j.sna.2019.06.038.
- [123] Subramanyam P, Khan T, Neeraja Sinha G, Suryakala D, Subrahmanyam C. Plasmonic Bi nanoparticle decorated BiVO4/rGO as an efficient photoanode for photoelectrochemical water splitting. Int J Hydrog Energy. 2020;45:7779-87. doi: 10.1016/j.ijhydene.2019.08.214.
- [124] Li P, Zhu L, Ma C, Zhang L, Guo L, Liu Y, et al. Plasmonic molybdenum tungsten oxide hybrid with surface-enhanced raman scattering comparable to that of noble metals. ACS Appl Mater Interfaces. 2020;12:19153-60. doi: 10.1021/ acsami.0c00220.
- [125] Odda AH, Xu Y, Lin J, Wang G, Ullah N, Zeb A, et al. Plasmonic MoO3-x nanoparticles incorporated in Prussian blue frameworks exhibit highly efficient dual photothermal/photodynamic therapy. J Mater Chem B. 2019;7:2032-42. doi: 10.1039/c8tb03148g.

- [126] Zeng J, Xuan Y. Tunable full-spectrum photo-thermal conversion features of magnetic-plasmonic Fe3O4/TiN nanofluid. Nano Energy. 2018;51:754-63. doi: 10.1016/ j.nanoen.2018.07.034.
- [127] He J, Ai L, Liu X, Huang H, Li Y, Zhang M, et al. Plasmonic CuS nanodisk assembly based composite nanocapsules for NIRlaser-driven synergistic chemo-photothermal cancer therapy. J Mater Chem B. 2018;6:1035-43. doi: 10.1039/ c7tb02772a.
- [128] Guo L, Yin H, Xu M, Zheng Z, Fang X, Chong R, et al. In situ generated plasmonic silver nanoparticle-sensitized amorphous titanium dioxide for ultrasensitive photoelectrochemical sensing of formaldehyde. ACS Sens. 2019:4:2724-9. doi: 10.1021/acssensors.9b01204.
- [129] Giovannini G, Ardini M, Maccaferri N, Zambrana-Puyalto X, Panella G, Angelucci F, et al. Bio-assisted tailored synthesis of plasmonic silver nanorings and site-selective deposition on graphene arrays. Adv Optical Mater. 2020;8:1901583. doi: 10.1002/adom.201901583.
- [130] Cho NH, Byun GH, Lim YC, Im SW, Kim H, Lee HE, et al. Uniform chiral gap synthesis for high dissymmetry factor in single plasmonic gold nanoparticle. ACS Nano. 2020;14:3595-602. doi: 10.1021/acsnano.9b10094.
- Li W, Xu J, Zhou Q, Wang S, Feng Z, Hu D, et al. Bidirectional plasmonic coloration with gold nanoparticles by wavelengthswitched photoredox reaction. Nanoscale. 2018;10:21910-7. doi: 10.1039/c8nr05763j.
- Liu Y, Pan M, Wang W, Jiang Q, Wang F, Pang DW, et al. [132] Plasmonic and photothermal immunoassay via enzyme-triggered crystal growth on gold nanostars. Anal Chem. 2019;91:2086-92. doi: 10.1021/acs.analchem.8b04517.
- [133] Singh P, König TAF, Jaiswal A. NIR-active plasmonic gold nanocapsules synthesized using thermally induced seed twinning for surface-enhanced raman scattering applications. ACS Appl Mater Interfaces. 2018;10:39380-90. doi: 10.1021/acsami.8b14445.
- [134] Pinheiro PC, Fateixa S, Daniel-da-Silva AL, Trindade T. An integrated approach for trace detection of pollutants in water using polyelectrolyte functionalized magneto-plasmonic nanosorbents. Sci Rep. 2019;9:1-14. doi: 10.1038/s41598-019-56168-6.
- [135] Al Mubarak ZH, Premaratne G, Dharmaratne A, Mohammadparast F, Andiappan M, Krishnan S. Plasmonic nucleotide hybridization chip for attomolar detection: Localized gold and tagged core/shell nanomaterials. Lab a Chip. 2020;20:717-21. doi: 10.1039/c9lc01150a.
- [136] Younis MR, Wang C, An R, Wang S, Younis MA, Li ZQ, et al. Low power single laser activated synergistic cancer phototherapy using photosensitizer functionalized dual plasmonic photothermal nanoagents. ACS Nano. 2019;13:2544-57. doi: 10.1021/acsnano.8b09552.
- [137] Shahine I, Jradi S, Beydoun N, Gaumet JJ, Akil S. Plasmonenhanced photoluminescence and photocatalysis reactions in metal-semiconductor nanomaterials: UV-generated hot electron in gold-zinc oxide. ChemPhotoChem. 2020;4:181-94. doi: 10.1002/cptc.201900252.
- [138] Shehata N, Samir E, Kandas I. Plasmonic-ceria nanoparticles as fluorescence intensity and lifetime quenching optical sensor. Sens (Switz). 2018;18:1-9. doi: 10.3390/s18092818.

- [139] Li J, Koo KM, Wang Y, Trau M. Native microRNA targets trigger self-assembly of nanozyme-patterned hollowed nanocuboids with optimal interparticle gaps for plasmonic-activated cancer detection. Small. 2019;15:1904689. doi: 10.1002/ smll.201904689.
- [140] Thangamuthu M, Santschi C, Martin OJF. Photocatalytic ammonia production enhanced by a plasmonic near-field and hot electrons originating from aluminium nanostructures. Faraday Discuss. 2019;214:399-415. doi: 10.1039/ c8fd00146d.
- [141] Etman AS, Wang L, Edström K, Nyholm L, Sun J. Molybdenum oxide nanosheets with tunable plasmonic resonance: aqueous exfoliation synthesis and charge storage applications. Adv Funct Mater. 2019;29:1-13. doi: 10.1002/ adfm.201806699.
- [142] Pathak TK, Swart HC, Kroon RE. Structural and plasmonic properties of noble metal doped ZnO nanomaterials. Phys B: Condens Matter. 2018;535:114-8. doi: 10.1016/ j.physb.2017.06.074.
- [143] Yoshino M, Kubota Y, Nakagawa Y, Terano M. Efficient fabrication process of ordered metal nanodot arrays for infrared plasmonic sensor. Micromachines. 2019;10:27-30. doi: 10.3390/mi10060385.
- [144] Guo Y, Khan AU, Cao K, Liu G. Janus plasmonic silver nanoplatelets for interface stabilization. ACS Appl Nano Mater. 2018;1:5377-81. doi: 10.1021/acsanm.8b01141.
- Koneti S, Borges J, Roiban L, Rodrigues MS, Martin N, Epicier T, et al. Electron tomography of plasmonic Au nanoparticles dispersed in a TiO 2 dielectric matrix. ACS Appl Mater Interfaces. 2018;10:42882-90. doi: 10.1021/ acsami.8b16436.
- [146] Lee JW, Jung H, Cho HH, Lee JH, Nam Y. Gold nanostarmediated neural activity control using plasmonic photothermal effects. Biomaterials. 2018;153:59-69. doi: 10.1016/ i.biomaterials.2017.10.041.
- Runowski M, Stopikowska N, Goderski S, Lis S. Luminescentplasmonic, lanthanide-doped core/shell nanomaterials modified with Au nanorods - Up-conversion luminescence tuning and morphology transformation after NIR laser irradiation. J Alloy Compd. 2018;762:621-30. doi: 10.1016/ j.jallcom.2018.05.211.
- [148] Cao M, Liu Q, Chen M, Chen L, Yang D, Hu H, et al. Fully alloying AuAg nanorods in a photothermal nano-oven: superior plasmonic property and enhanced chemical stability. ACS Omega. 2018;3:18623-9. doi: 10.1021/ acsomega.8b03020.
- [149] Clarke C, Liu D, Wang F, Liu Y, Chen C, Ton-That C, et al. Large-scale dewetting assembly of gold nanoparticles for plasmonic enhanced upconversion nanoparticles. Nanoscale. 2018;10:6270-6. doi: 10.1039/c7nr08979a.
- Dal'Toé ATO, Colpani GL, Padoin N, Fiori MA, Soares C. Lanthanum doped titania decorated with silver plasmonic nanoparticles with enhanced photocatalytic activity under UV-visible light. Appl Surf Sci. 2018;441:1057-71. doi: 10.1016/j.apsusc.2018.01.291.
- [151] Sang L, Zhang S, Zhang J, Yu Z, Bai G, Du C. TiO2 nanotube arrays decorated with plasmonic Cu, CuO nanoparticles, and eosin Y dye as efficient photoanode for water splitting. Mater Chem Phys. 2019;231:27-32. doi: 10.1016/ j.matchemphys.2019.04.018.

- Kong T, Zhang C, Gan X, Xiao F, Li J, Fu Z, et al. Fast transformation of a rare-earth doped luminescent sub-microcrystal: Via plasmonic nanoislands. J Mater Chem C. 2020;8:4338-42. doi: 10.1039/d0tc00060d.
- [153] Novoselov KS, Geim AK, Morozov SV, Jiang D, Zhang Y, Dubonos SV et al. Electric field effect in atomically thin carbon films. Science. 2004;306:666-9. doi: 10.1126/science.1102896.
- [154] Kanidi M, Dagkli A, Kelaidis N, Palles D, Aminalragia-Giamini S, Marquez-Velasco J, et al. Surface-enhanced raman spectroscopy of graphene integrated in plasmonic silicon platforms with three-dimensional nanotopography. J Phys Chem C. 2019;123:3076-87. doi: 10.1021/acs.jpcc.8b10356.
- [155] Wang M, Yin H, Yu T, Tan LS, Urbas A, Chiang LY. Reversible enlargement of photoswitchable dielectric properties by plasmonic [60]fullerenyl core-shell nanoparticles on graphene nanosheets. J Phys Chem C. 2020;124:5759-71. doi: 10.1021/acs.jpcc.9b10102.
- [156] Hou S, Yan J, Hu Z, Wu X. Enhancing the plasmonic circular dichroism by entrapping chiral molecules at the core-shell interface of rod-shaped Au@Ag nanocrystals. Chem Commun. 2016;52:2059-62. doi: 10.1039/c5cc08505e.
- [157] Chauhan DS, Kumawat MK, Prasad R, Reddy PK, Dhanka M, Mishra SK, et al. Plasmonic carbon nanohybrids for repetitive and highly localized photothermal cancer therapy. Colloids Surf B: Biointerfaces. 2018;172:430-9. doi: 10.1016/ j.colsurfb.2018.08.054.
- [158] Devi P, Hipp KN, Thakur A, Lai RY. Waste to wealth translation of e-waste to plasmonic nanostructures for surfaceenhanced Raman scattering. Appl Nanosci (Switz). 2020;10:1615-23. doi: 10.1007/s13204-020-01273-6.
- [159] Allsop T, Arif R, Neal R, Kalli K, Kundrát V, Rozhin A, et al. Photonic gas sensors exploiting directly the optical properties of hybrid carbon nanotube localized surface plasmon structures. Light: Sci Appl. 2016;5:e16036. doi: 10.1038/ Isa.2016.36.
- [160] Qiu W, Chen H, Ren J, Qiu P, Lin Z, Wang J, et al. Symmetrybreaking effect on the electromagnetic properties of plasmonic trimers composed of graphene nanodisks. Appl Sci (Switz). 2018;8:374. doi: 10.3390/app8030374.
- [161] Chuntonov L, Haran G. Trimeric plasmonic molecules: the role of symmetry. Nano Lett. 2011;11:2440-5. doi: 10.1021/nl2008532.
- [162] Chuntonov L, Haran G. Effect of symmetry breaking on the mode structure of trimeric plasmonic molecules. J Phys Chem C. 2011;115:19488-95. doi: 10.1021/jp2045433.
- [163] Chuntonov L, Haran G. Optical activity in single-molecule surface-enhanced Raman scattering: Role of symmetry. MRS Bull. 2013;38:642-7. doi: 10.1557/mrs.2013.159.
- [164] Wang J, Xu H, Li S, Yan B, Shi Y, Wang C, et al. Plasmonic and photo-electrochemical enhancements of the AuAg@Au/RGO-C3N4 nanocomposite for the detection of da. Analyst. 2017;142:4852-61. doi: 10.1039/c7an01561e.
- [165] Cheung W, Patel M, Ma Y, Chen Y, Xie Q, Lockard JV, et al. π -Plasmon absorption of carbon nanotubes for the selective and sensitive detection of Fe3 + ions. Chem Sci. 2016;7:5192-9. doi: 10.1039/c6sc00006a.
- [166] Shahine I, Jradi S, Beydoun N, Gaumet JJ, Akil S. Plasmonenhanced photoluminescence and photocatalysis reactions in metal-semiconductor nanomaterials: UV-generated hot electron in gold-zinc oxide. ChemPhotoChem. 2020;4:181194. doi: 10.1002/cptc.201900252.

- [167] Yang J, Liu Z, Hu Z, Zeng F, Zhang Z, Yao Y, et al. Enhanced single-mode lasers of all-inorganic perovskite nanocube by localized surface plasmonic effect from Au nanoparticles. J Lumin. 2019;208:402-7. doi: 10.1016/j.jlumin.2018.12.055.
- [168] Prusty G, Lee JT, Seifert S, Muhoberac BB, Sardar R. Ultrathin plasmonic tungsten oxide quantum wells with controllable free carrier densities. J Am Chem Soc. 2020;142:5938-42. doi: 10.1021/jacs.9b13909.
- [169] Mezni A, ben Saber N, Bukhari A, Ibrahim MM, Al-Talhi H, Alshehri NA, et al. Plasmonic hybrid platinum-titania nanocomposites as highly active photocatalysts: Self-cleaning of cotton fiber under solar light. J Mater Res Technol. 2020;9:1447-56. doi: 10.1016/j.jmrt.2019.11.070.
- [170] Fan H, Li Y, Liu J, Cai R, Gao X, Zhang H, et al. Plasmonenhanced oxidase-like activity and cellular effect of Pdcoated gold nanorods. ACS Appl Mater Interfaces. 2019;11:45416-26. doi: 10.1021/acsami.9b16286.
- [171] Yuan G, Ping C, Zhao Q, Cao M, Jin Y, Ge C. Surface reconstruction for preparation of plasmonic Au/TiO 2 nanoparticle with perfect hetero interface and improved photocatalytic capacity. J Nanosci Nanotechnol. 2017;18:5088-94. doi: 10.1166/jnn.2018.15331.
- $\ensuremath{[172]}$ Smith KJ, Cheng Y, Arinze ES, Kim NE, Bragg AE, Thon SM. Dynamics of energy transfer in large plasmonic aluminum nanoparticles. ACS Photonics. 2018;5:805-13. doi: 10.1021/ acsphotonics.7b00932.